11

Mathematical Modeling of Syk Activation in Allergen-Stimulated Mast Cells and Basophils

Ambarish Nag[1]*, Michael I. Monine[1]†, Byron Goldstein[1],
James R. Faeder[2] and Michael L. Blinov[3]
[1]*Los Alamos National Laboratory*
[2]*University of Pittsburgh School of Medicine*
[3]*University of Connecticut School of Medicine*
U.S.A.

1. Introduction

Mast cells and basophils play major roles in allergic responses of the immediate type (Rivera & Gilfillan, 2006). Allergic individuals produce IgE that is specific for the multivalent foreign molecules (allergens) that trigger their allergic responses. IgE binds with high affinity through its constant region to a monovalent receptor, FcϵRI, that is expressed on the surface of basophils and mast cells and that mediates much of mast cell activation in allergic reactions. Upon exposure to the allergen, the bridging of multiple IgEs by the allergen results in the aggregation of FcϵRI receptors on the cell surface, which in turn triggers a cascade of biochemical reactions that results in the release of preformed mediators from granules together with the synthesis and release of lipid mediators and cytokines. The cytosolic protein tyrosine kinase Syk plays a crucial role in FcϵRI-mediated signaling cascade in mast cells. A clone of the *syk* gene was first isolated on the basis of partial sequenced information of a 40 kDa kinase from porcine spleen (de Castro, 2011; Taniguchi et al., 1991). The product of this gene was identified as a nonreceptor-type protein tyrosine kinase of 72 kDa (Yang et al., 1994) and was named Spleen Tyrosine Kinase (Syk). Syk has two Src-homology 2 domains (SH2) which are separated by a linker region from the kinase domain (Siraganian et al., 2002). FcϵRI is a tetrameric complex composed of an α-chain that binds IgE to form a long-lived complex, and three subunits, a β-chain and two disulfide-linked γ-chains (Blank et al., 1989) that contain immunoreceptor tyrosine-based activation motifs (ITAMs). The FcϵRI receptor lacks intrinsic enzymatic acitivity and requires non-receptor protein tyrosine kinase activity in propagating cellular signals in allergen-stimulated mast cells and basophils. The unphosphorylated β-chain of the FcϵRI receptor associates weakly with the Src family kinase Lyn, which is anchored to the inner layer of the plasma membrane (Vonakis et al., 1997; 2001). Upon receptor aggregation, Lyn transphosphorylates tyrosines in the β and γ ITAMs. Syk from the cytosol binds with high affinity through its two SH2 domains to the doubly phosphorylated γ ITAM (Benhamou et al., 1993; Hutchcroft et al., 1992). Recent experimental

*Currently at National Renewable Energy Laboratory, U.S.A.
†Currently at Novartis Institutes for Biomedical Research, Inc., U.S.A.

findings (de Castro et al., 2010; Siraganian et al., 2010) indicate that the binding of Syk to phosphorylated γ ITAM causes a conformational change of the Syk molecule and enhances its enzymatic activity. The conformation change of the activated Syk molecule exposes its COOH-terminal region, thereby enabling the phosphorylation of two conserved tyrosines (Tyr-624 and Tyr-625 in rat Syk). These two phosphotyrosines maintain the γ ITAM bound Syk in an open conformation, which allows the phosphorylation on multiple tyrosines by both Lyn and Syk (Siraganian et al., 2002), with a second Syk molecule playing the major role in transphosphorylating two tyrosines, Tyr-519 and Tyr-520, in the Syk activation loop (Zhang et al., 2000; 1998). This yields a fully activated Syk that phosphorylates the adaptor proteins LAT (Linker for Activation of T cells) and NTAL (Non-T-cell Activation Linker) that function as scaffolds, organizing other signaling proteins that are responsible for signaling events further downstream (Rivera, 2005). The phosphorylation of the two tyrosine residues in the activation loop of Syk is critical to the propagation of FcϵRI signaling, since the substitution of these tyrosines by phenylalanine abrogates signaling and degranulation in mast cells (Zhang et al., 1998).

In order to predict the strength of the allergen-induced signaling in mast cells and basophils, it is important to understand the subtle kinetic effects underlying Syk activation, and how these kinetic effects influence the level of Syk activation, since this event couples the initial signaling events in the cascade with the downstream signaling events. Although many of the biochemical reactions leading from Syk activation to histamine release have been investigated in great detail, a complete model of the signaling cascade still eludes us. A detailed mathematical model of the early signaling events, up to and including Syk activation, that are triggered when IgE-FcϵRI complexes are exposed to a bivalent or trivalent ligand on rat basophilic leukemia (RBL) cells has been developed by Faeder et al. (2003). In the model, full activation of a Syk molecule requires its transphosphorylation by a second Syk molecule, the two Syk molecules being bound to different receptors in a receptor dimer (Zhang et al., 2000). In this chapter, we review our research (Nag, Faeder & Goldstein, 2010; Nag, Monine, Blinov & Goldstein, 2010) on the exploration of the different factors that influence the kinetics and the level of Syk activation in stimulated mast cells and basophils using the mathematical model of Faeder et al. (2003).

First, we use the model of Faeder et al. (2003) to investigate investigate the effects of the extracellular allergen concentration and the cellular FcϵRI and Syk expression levels on the extent of Syk activation. Using model simulations, we explore how the extent of Syk activation varies as a function of the concentration of the allergen, for given FcϵRI and Syk concentrations, and for a given set of kinetic parameters characterizing binding, unbinding, phosphorylation and dephosphorylation events (Nag, Faeder & Goldstein, 2010).

For bivalent allergens binding to the monovalent IgE-FcϵRI complex, a plot of the equilibrium concentration of receptors in aggregates versus the log of the free allergen concentration, the cross-linking curve, is symmetric and bell-shaped. One might naively expect that the variation of Syk activation with the equilibrium allergen concentration should be qualitatively similar to the variation in the number of cross-linked FcϵRI receptors. We define the Syk activation curve as a plot of the number of fully activated Syk molecules in a cell versus the log of the equilibrium free allergen concentration. Our model predicts that if the mechanism by which Syk is fully activated involves the transphosphorylation of Syk by Syk, then Syk activation curves can be either bell-shaped or double humped, depending on the relative cellular concentrations of Syk and FcϵRI. For many physiological Syk expression levels, the

predicted Syk activation curve follows the receptor cross-linking curve. However, for limiting Syk concentration, an excess of cross-linked receptors over Syk molecules over a range of free equilibrium allergen concentrations can occur and result in high-dose inhibition of Syk activation (Hlavacek et al., 2003). At other allergen concentrations, the extent of cross-linking is lower so that there is enough Syk for two Syk molecules to be bound to the same receptor dimer. This predicted differential behavior at different allergen concentrations gives rise to the variable shape (unimodal/multimodal) of the Syk activation curve (Hlavacek et al., 2003). More interestingly, for some reasonable parameter regimes, the bimodal Syk activation curves can be non-symmetric with respect to the ligand concentration. We discuss how, even though it is only receptor aggregates that trigger responses, differences in total ligand concentration, that are not reflected in the extent of receptor aggregation, can lead to subtle kinetic effects that yield qualitative differences in the levels of Syk activation.

Secondly, we use our mathematical model to evaluate the role of serial engagement (Davis, 1995; Valitutti et al., 1995) in Syk activation in mast cells (Nag, Monine, Blinov & Goldstein, 2010). The terms serial triggering and serial engagement were introduced in immunology when Valitutti et al. (Davis, 1995; Valitutti et al., 1995) reported that within the contact area between an antigen presenting cell (APC) and a T cell, a few antigenic peptides bound to major histocompatibility complex molecules (pMHC) mediated the internalization of hundreds of T cell receptors (TCRs). The concept of serial engagement was introduced to describe the ability of a single peptide, bound to a MHC molecule, to sequentially interact with TCRs within the contact region between a T cell and an APC.

The observation that TCRs undergo serial engagement, coupled with the kinetic proofreading model for cell signaling (Goldstein et al., 2008; McKeithan, 1995), led to the hypothesis that for T cell activation there should be an optimal range of half-lives for the pMHC-TCR bond (Lanzavecchia et al., 1999). The basic idea of kinetic proofreading is that for a TCR to become activated it must remain associated with a pMHC long enough for a set of biochemical modifications to occur. In case of dissociation of the pMHC from the TCR before the necessary modifications have been completed, signaling is frustrated and activation is not achieved. In order to obtain a measurable signaling response from a T cell, multiple TCRs must be activated. Therefore, at low pMHC density, a single pMHC needs to trigger multiple TCR before it diffuses out of the contact region. If the pMHC dissociates too rapidly it will encounter many TCRs but activate only a few. On the other hand, if it remains bound too long it will activate those it encounters but the frequency of encounters will be small. The recognition that the pMHC-TCR bond half-life has opposing effects on kinetic proofreading and serial engagement led to the prediction that to achieve an optimal rate of TCR activation there should be an optimal half-life, or equivalently an optimal dissociation rate constant k_{off}, (Coombs & Goldstein, 2005; Lanzavecchia et al., 1999). Although some studies have found an optimal half-life for T cell activation (Carreno et al., 2007; Coombs et al., 2002; Kalergis et al., 2001), there are other results that are not consistent with this model (reviewed in (Aleksic et al., 2010; Stone et al., 2009)).

In addition to surface ligands, soluble multivalent ligands can serially engage cell surface receptors involving repeated binding and dissociating of ligand sites from receptors before all ligand sites become free and the ligand leaves the surface. Although there has been a significant effort directed at unraveling the role of serial engagement of TCRs in activating T-cells, the role of serial engagement by soluble multivalent ligands, of other multichain immune recognition receptors in cell activation has remained largely unexplored.

The immunological term avidity was coined more than fifty years ago to distinguish between the binding properties of an antibody and its monovalent Fab fragment (reviewed in (Karush, 1989)). It was observed that an IgG, at low concentrations, could bind to a surface containing multiple binding sites (epitopes) with an apparent affinity that was orders of magnitude greater than the equilibrium constant for binding of one of its Fab sites to an epitope (Gopalakrishnan & Karush, 1974; Greenbury et al., 1965; Hornick & Karusch, 1972). Avidity arises when the density of surface binding sites is sufficiently high that multivalent ligands are observed to dissociate from the surface more slowly than their monovalent constituent parts, thus exhibiting a high apparent affinity. When a site on a doubly bound IgG dissociates, the epitope it was bound to will diffuse away. If this newly freed site on the IgG binds to another epitope before its second site dissociates, the IgG will remain bound to the surface. Thus, avidity can arise by ligands serially engaging epitopes, traversing from epitope to epitope, along the surface.

Avidity can arise in another way that does not require serial engagement. For example, the cross-linking IgE-FcϵRI complexes on rat basophilic leukemia (RBL) cells by a highly multivalent antigen leads to the rapid formation of large stable aggregates of immobilized receptors (Andrews et al., 2008; Menon et al., 1986). This observation suggests the possibility that a site on a bound ligand can dissociate from, and rebind to the same immobilized receptor many times, effectively increasing its off rate constant, before all its sites on the ligand become free and the ligand dissociates from the cell. Recent multi-color tracking experiments indicate that small aggregates of IgE-FcϵRI complexes, comprising two to four receptors, remain mobile on the RBL surface even at ligand doses that result in degranulation (Andrews et al., 2009).

A major difficulty in assessing the role of serial engagement of receptors in cell signaling is that the phenomena cannot be studied in isolation. To gauge the role of serial engagement in mast cell signaling, we use the detailed mathematical model of the early events triggered when IgE-FcϵRI complexes are exposed to a bivalent or trivalent ligand on RBL cells (Faeder et al., 2003). Simulations using this model has enabled us to delineate how different alterations in the binding properties of the ligand, that result in the same rates of serial engagement of receptors, can alter receptor activation in different ways.

2. Mathematical model

2.1 Components

We briefly review our mathematical model for the early signaling events initiated by ligand-induced aggregation of FcϵRI-IgE complexes on mast cells and basophils. The model is summarized in Fig. 1. The external stimulus in the model is constituted by a symmetric bivalent ligand, such as a monoclonal anti-IgE, that cross-links two IgE molecules, each bound to a FcϵRI receptor. We assume that aggregates of receptors are limited to dimers. The tetrameric FcϵRI is modeled as three subunits, with the disulphide-bonded pair of γ chains treated as one unit. The extracellular region of the α chain binds to the Fc portion of IgE. The binding of IgE to the α subunit of the FcϵRI receptor is not explicitly considered, as the half-life for the dissociation of the IgE-FcϵRI complex is much longer than the processes we consider (Kulczycki & Metzger, 1974). We therefore ignore dissociation and treat the IgE-FcϵRI complex as a single unit which we refer to as the receptor.

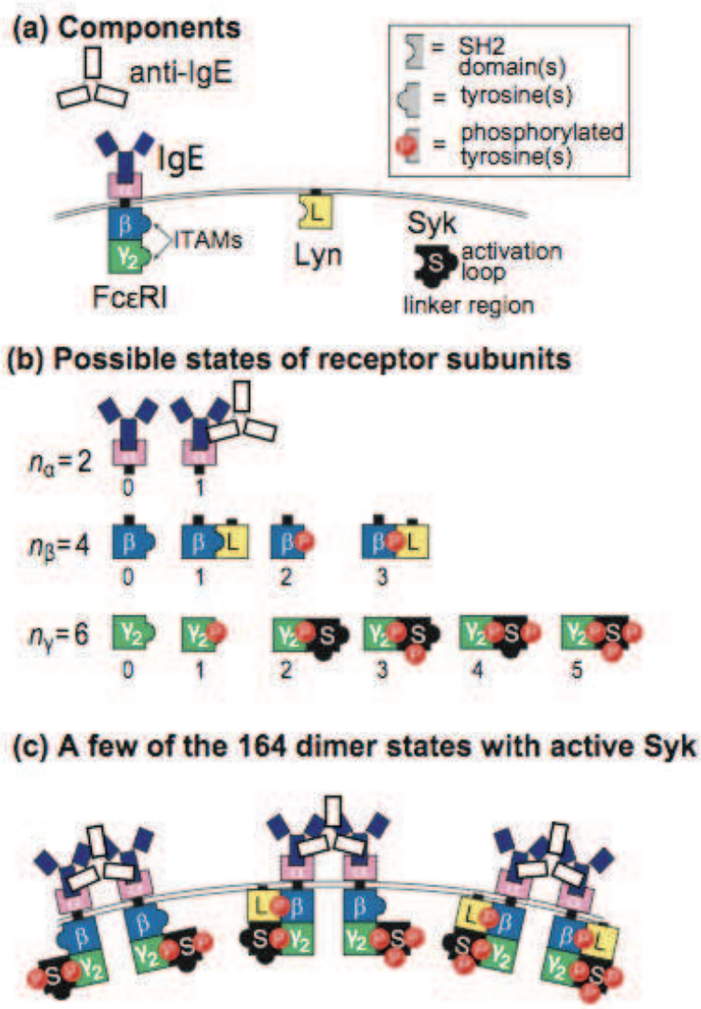

Fig. 1. Components and states of the model, modified from Faeder et al. (2003). The bivalent ligand is a monoclonal anti-IgE that can dimerize receptors.

The β subunit and the γ dimer contain the ITAMs that, upon phosphorylation, become binding sites for the SH2 domains of the two kinases, Lyn and Syk. A simplifying assumption of our model is that multiple tyrosine residues on receptor subunits and Syk are treated as single units of phosphorylation, as indicated in Fig. 1a. For example, the separate tyrosines in the β ITAM are lumped together, as are those in the γ ITAM, so that in the model an ITAM is either phosphorylated or unphosphorylated. Sites of Syk tyrosine phosphorylation are lumped into two units: the activation loop, which is phosphorylated by Syk, and the linker region, which is phosphorylated by Lyn. Fig. 1b shows the states of the β chain and the lumped γ chains included in the model. Each unit can be phosphorylated or unphosphorylated, and can be associated with a kinase in any of several states. In the model, each β chain and γ dimer can bind only a single kinase molecule at a time.

The model permits a large number of receptor states (Figs. 1b and 1c). Since the state of each subunit is independent of the states of the other subunits, the total number of monomer

states is $n_\alpha n_\beta n_\gamma = 48$. When a monovalent ligand is present as well as a bivalent ligand, the number of monomeric states increases to 72. In a dimer, each subunit must be engaged with the ligand, so the total number of dimer states is $n_\beta n_\gamma (n_\beta n_\gamma + 1)/2 = 300$. In addition, there are six nonreceptor states, free ligand, free Lyn, and Syk in each of its four possible states of phosphorylation, to yield a total of 354 distinct chemical species in the model. Our model is composed of 354 chemical species and the 3680 chemical reactions that connect them. (For details of the chemical reactions see Fig. 2 in Faeder et al. (2003).)

2.2 Network structure and parameters

The required input for the model are the rate constants associated with each of the reactions, as well as the initial concentrations of each of the components, which are specific to the cell type being modeled. We consider a bivalent allergen that differs from the ligand used by Faeder et al. (2003) in that it binds reversibly to the receptor. Other than a different bivalent ligand, the current reaction network is the same as in Faeder et al. (2003). Lyn can associate with a receptor in a dimer in two possible ways, weakly with the unphosphorylated β chain of the receptor and strongly to the phosphorylated β ITAM. Syk associates with FcϵRI through an interaction between its tandem SH2 domains and the doubly phosphorylated γ ITAM. Lyn, associated with a receptor aggregate, can transphosphorylate the β and γ ITAMs on an adjacent receptor. In the model, all Lyn molecules available to the receptor are in an active form. The available Lyn is considerably less than the total cellular Lyn. Syk is phosphorylated in the model by either Lyn or Syk through transphosphorylation. Lyn phosphorylates Syk tyrosines located in the linker region, while Syk phosphorylates the activation loop tyrosines. Although Lyn may be responsible *in vivo* for a small portion of the Syk activation loop phosphorylation, full Syk activation loop phosphorylation requires kinase-active Syk (Hong et al., 2002).

In the model, phosphorylated units that are not protected through association with an SH2 domain can be dephosphorylated with a common rate constant, d, termed the intrinsic rate constant for dephosphorylation. Dephosphorylation is blocked when an SH2 domain is associated with the phosphorylated site. At long times, the model system goes to a steady state, not an equilibrium. In the model, tyrosines are constantly being phosphorylated and dephosphorylated. As a result, maintaining a constant level of phosphorylation requires a constant input of energy. Since the modifications of the intracellular domains of the receptors do not influence the extracellular binding, the distribution of ligand-receptor aggregates goes to the same equilibrium as would be obtained if no chemical modifications occurred.

2.3 Implementation of rule-based modeling

The reaction rules and their associated rate constants were specified in the syntax of the second-generation version of BioNetGen (Blinov et al., 2004; Faeder et al., 2009), which uses graph theoretic methods to automatically generate the associated network of kinetic balances (ordinary differential equations). The open-source software (available through http://bionetgen.org) uses standard numerical algorithms to solve the generated system of equations and obtain the time courses of all the species until the system attains a steady state. In our simulations, all the kinetic parameters except the ones related to ligand binding and unbinding are taken from Faeder et al. (2003), where a complete discussion of how the parameters were obtained is given.

3. The role of cellular FcεRI and Syk expression levels in determining the Syk activation response to extracellular stimulation of mast cells and basophils

In the current investigation we model the Syk dose-response curves in human basophils. A broad distribution of Syk expression levels in human basophils, ranging from 5000 to 60,000 molecules per cell, has been reported in a recent survey (MacGlashan Jr, 2007). MacGlashan and co-workers have observed that a low expression level of Syk attenuates the calcium response (MacGlashan Jr & Lavens-Phillips, 2001), an event which is more proximal to Syk activation in the signaling cascade than histamine release. Maximal histamine release from human basophils shows a strong correlation with Syk activation (MacGlashan Jr, 2007). The number of FcεRI per human basophil varies from 1000 to 1000,000 with a typical value of about 100,000 FcεRI (MacGlashan Jr, 2007). Experimental observations (MacGlashan Jr, 2007) suggest that the median Lyn expression level in human basophils is about 100,000 molecules per cell. Using simulations of the detailed model, we examine the Syk activation curve for different sets of receptor and Syk expression levels, keeping the available Lyn fixed at 100,000 per cell.

3.1 The shape of the Syk activation curve is predicted to depend on the abundance of Syk relative to the number of FcεRI

At equilibrium, the receptor cross-linking curve is always symmetric and bell shaped (Dembo & Golstein, 1978). The shape of the Syk activation curve is predicted to depend on the concentrations of Syk and FcεRI receptors. The number of FcεRI per human basophils varies from 10^3 to 10^6 with a typical value of about 100,000 FcεRI (MacGlashan Jr, 2007). The corresponding Syk concentration ranges from 5×10^3 to 6×10^4 per cell (MacGlashan Jr, 2007). At the lower boundary of the range (5×10^3 Syk per cell), a receptor population of 7×10^4 per cell results in a predicted bimodal Syk activation curve (Fig. 2a). At the upper boundary (6×10^4 Syk per cell), the same level of receptors results in a bell-shaped Syk activation curve (Fig. 2b).

In the model, full activation of a Syk molecule requires its transphosphorylation by a second Syk, which occurs when two Syk molecules are bound to different receptors cross-linked by a bivalent ligand. We refer to a receptor dimer with two bound Syk molecules, one on each receptor, as a Syk dimer. Formation of Syk dimers is essential for Syk activation. Double humped Syk activation curves are predicted to occur (Fig. 2a) if the concentration of receptors dimers becomes sufficiently high that the number of receptor dimers with two Syks bound decreases with increasing receptor dimer concentration.

Studies of histamine release dose response curves (log-log plots of the fraction of a cell's total histamine released in a given time versus the concentration of ligand the cell is exposed to) lead to the definition of two types of inhibition of histamine release. In Type I inhibition, commonly known as antigen excess inhibition, histamine release is inhibited when receptor crosslinks are decreased. In the more interesting Type II inhibition, histamine release is inhibited when receptor crosslinks are increased. This type of inhibition was first observed by Becker et al. (Becker et al., 1973) who exposed human basophils to anti-IgE and found that inhibition of histamine release was correlated with increased aggregation of IgE. Applying the same terminology for Syk activation, Type I inhibition occurs in our model for parameter regimes in which the number of Syk molecules is comparable to, or exceeds, the number of receptors in dimers, so that the dose-response curve (Syk activation curve) follows the

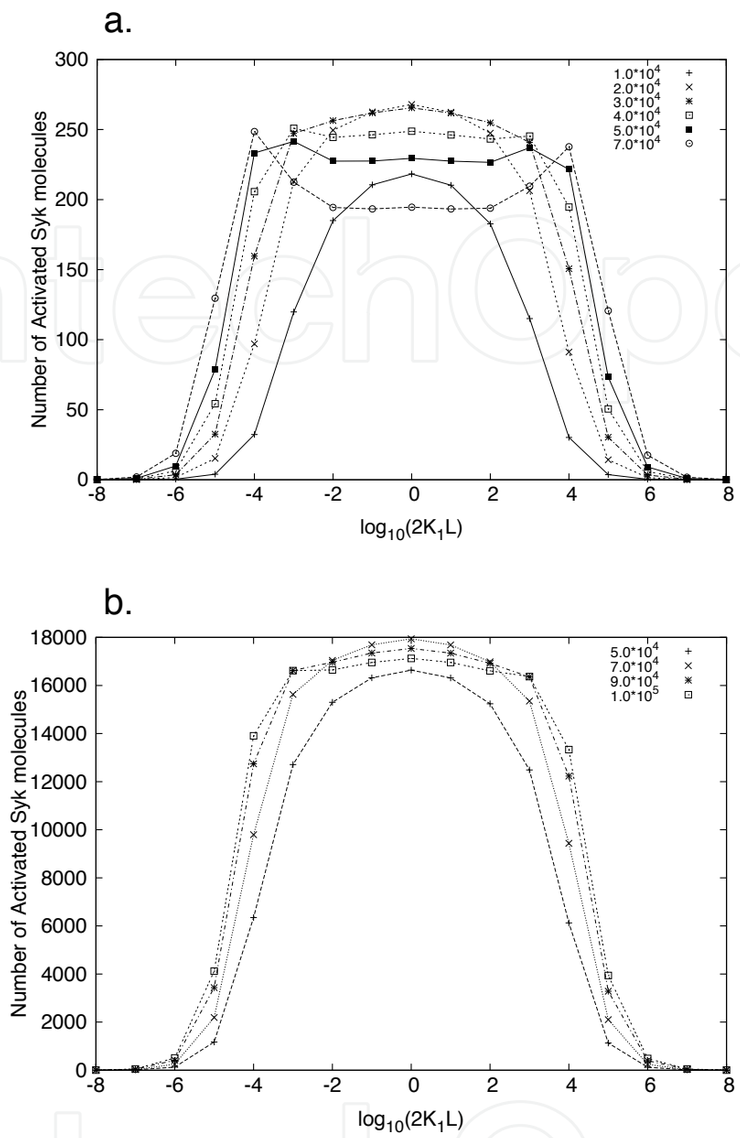

Fig. 2. Syk Activation curves for $k_{+1} = 2.5 \times 10^6$ $M^{-1}s^{-1}$, $k_{+2} = 8 \times 10^{-9}$ cm^2s^{-1}, $k_{-1} = k_{-2} = 0.01$ s^{-1}, and $[Lyn]_{tot} = 10^5$ per cell. Each curve corresponds to a different number of receptors per cell given in the legend. The number of activated Syk molecules on the y axis are given in numbers per cell. (a) $[Syk]_{tot} = 5 \times 10^3$ per cell; (b) $[Syk]_{tot} = 6 \times 10^4$ per cell. The number of activated Syk molecules on the y axis are the numbers per cell. In (a) the ratio of total receptors to total Syk varies from 2-14 while in (b) the same ratio varies from 0.83-1.67.

receptor cross-linking curve at all the ligand concentrations (Fig. 3a). This type of inhibition can be traced to the binding sites on IgE being blocked by the ligand at sufficiently high concentrations, so that the number of receptor cross-links is reduced. Type II inhibition in our model system results from an excess of FcϵRI-bound IgE dimers compared to the number of available Syk molecules, and is characterized by decreasing signaling response

(Syk activation) at ligand concentrations where receptor cross-linking is increasing. The reduction in Syk activation, with increasing ligand concentration, near the center of the Syk activation curve in Fig 3b is a Type II inhibition. Although we used a bivalent ligand in our simulations to illustrate the two types of inhibition, the valence of the ligand is not critical as long as it is multivalent.

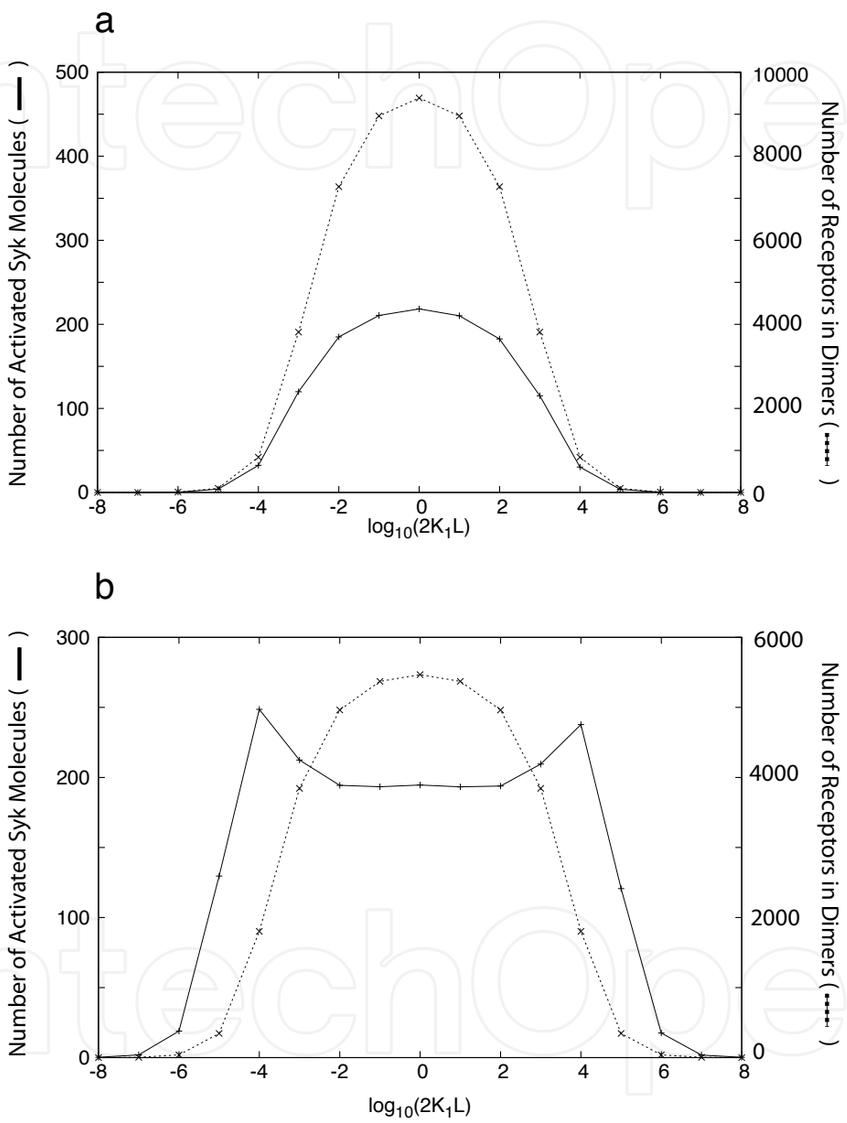

Fig. 3. Comparison of receptor cross-linking and Syk activation curves to determine the type of antigen excess inhibition. $k_{+1} = 2.5 \times 10^6 \mathrm{M}^{-1}\mathrm{s}^{-1}$, $k_{+2} = 8 \times 10^{-9}$ $\mathrm{cm}^2\mathrm{s}^{-1}$, $k_{-1} = k_{-2} = 0.01$ s^{-1}; $[\mathrm{Syk}]_{tot} = 5 \times 10^3$ per cell; $[\mathrm{Lyn}]_{tot} = 10^5$ per cell. (a) $[\mathrm{Fc}\epsilon\mathrm{RI}]_{tot} = 1 \times 10^4$. The dashed line represents (Number of receptors in dimers)/20.0 and the solid line represents the number of activated Syk molecules. (b) $[\mathrm{Fc}\epsilon\mathrm{RI}]_{tot} = 7 \times 10^4$. The dashed line represents (Number of receptors in dimers)/250.0 and the solid line represents the number of activated Syk molecules.

3.2 Effect of monovalent ligands on Syk activation

A way to distinguish between Type I and Type II inhibition is by comparing responses to anti-IgE in the presence and absence of Fab fragments (Magro & Alexander, 1974; Magro & Bennich, 1977). Adding monovalent ligand that competes for the same binding site as a multivalent ligand will always reduce the number of cross-links. Thus, if the response increases in the presence of monovalent ligand, the inhibition is Type II, while if it decreases it is of Type I. To demonstrate, we have incorporated monovalent ligand into the model, with the monovalent ligand having the same rate constants for binding and dissociation as a single anti-IgE Fab site. The reference case we use for studying the effects of adding monovalent ligands on the signaling response, measured by Syk activation in our model, is characterized by the parameter values $k_{-1} = k_{-2} = 0.01\text{s}^{-1}$, $k_{+1} = 2.5 \times 10^6$ M^{-1} s^{-1}, $k_{+2} = 8 \times 10^{-9}$ molecule^{-1} cm^2 s^{-1} and total Syk, Lyn and FcϵRI numbers per cell of 5×10^3, 1×10^5 and 1×10^5 respectively. We use this parameter set because it yields a bimodal Syk activation curve in the absence of the monovalent ligand. We add monovalent ligand to a maximum concentration of 6.6 nM which corresponds to 4×10^6 molecules per cell. We consider the effects of adding monovalent ligands on Syk activation at two bivalent ligand concentrations, 2×10^{-5} nM and 2×10^{-3} nM, corresponding to $2K_1L$ values of 10^{-5} and 10^{-3} respectively. Fig. 4 shows that adding monovalent IgE ligand in increasing concentrations leads to a gradual lowering in the Syk activation level at $2K_1L = 10^{-5}$ (Type I inhibition). In contrast, adding monovalent ligand in increasing concentrations at $2K_1L = 10^{-3}$ results in a gradual increase of the Syk activation level (Type II inhibition).

On plotting the Syk activation level as a function of the added monovalent ligand concentration for two values 10^{-5} and 10^{-3} of $2K_1L$, we obtain Fig. 4b which is qualitatively similar to the plot of histamine release as a function of the amount of added monomer anti-IgE (Fab) in Fig. 1 of Ref (Magro & Alexander, 1974) as shown in Fig. 4c. The similarity between the predicted variation of Syk activation and the experimentally observed variation of histamine release (Goldstein & Wofsy, 1994; Magro & Alexander, 1974) with added monomer concentration suggests one possible mechanism for Type II inhibition.

3.3 A symmetric cross-linking curve can lead to an asymmetric Syk activation curve

For the ligand-receptor binding parameters in Table 1, and FcϵRI and Syk concentrations of 1×10^5 and 7×10^3 per cell respectively, we observe a Syk activation curve with two prominent maxima at $2K_1L = 10^{-4}$ and $2K_1L = 10^4$ (Fig. 5a). This parameter set is used because it accentuates the asymmetry between the two maxima. The extent of receptor cross-linking at these two ligand concentrations are equal. The mean lifetime of the receptor dimer is independent of the ligand concentration, which implies that kinetic proofreading effects at these two ligand concentrations should be identical. Still, in the steady state, the model predicts that there is greater Syk activation at the lower ligand concentration ($2K_1L = 10^{-4}$), than at the higher ($2K_1L = 10^4$).

Even though all signaling events are initiated by receptor aggregation, it appears that the concentrations of free and bound receptors which are not in aggregates influence signaling. To investigate the origin of the asymmetry, we vary both the the ligand-IgE association (k_{+1}) and dissociation (k_{-1}) constants, such that the corresponding equilibrium constant K_1, and therefore the equilibrium cross-linking curve, remains unchanged. If the ligand-IgE dissociation constant is gradually reduced from 0.3 ($10^{-0.5}$) to 0.0003 ($10^{-3.5}$)s^{-1}, the Syk

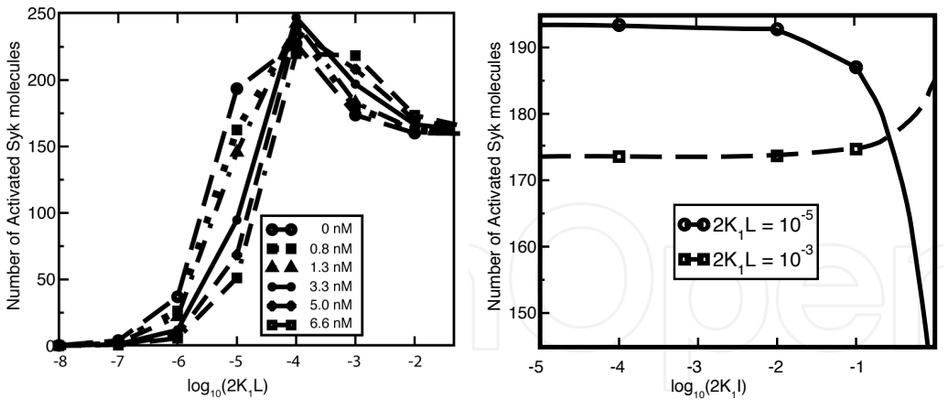

(a) (b)

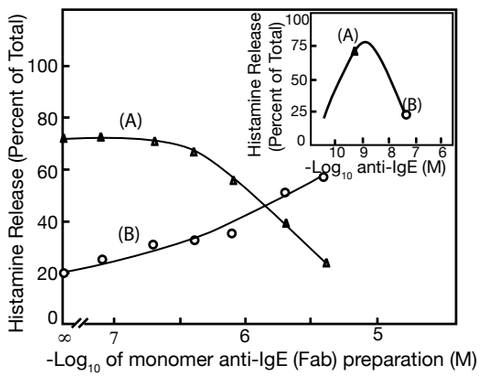

(c)

Fig. 4. (a)The effect of adding different concentrations of a monovalent IgE ligand on the extent of Syk activation at $2K_1L = 10^{-5}$ (Syk activation increases with $2K_1L$) and at $2K_1L = 10^{-3}$ (Syk activation decreases with $2K_1L$). The concentration of monovalent inhibitor (Fab fragments when the ligand is anti-IgE) present in the simulation is given in the figure. (b) The variation of the extent of Syk activation as a function of the concentration per cell of a monovalent inhibitor, I, at two ligand concentrations given by $2K_1L = 10^{-5}$ and $2K_1L = 10^{-3}$. The ligand-receptor binding parameters used are $k_{+1} = 2.5 \times 10^6$ $M^{-1}s^{-1}$, $k_{+2} = 8 \times 10^{-9}$ cm^2s^{-1}, $k_{-1} = k_{-2} = 0.01s^{-1}$. $[Syk]_{tot} = 5 \times 10^3$ per cell; $[Lyn]_{tot} = 10^5$ per cell; $[Fc\epsilon RI]_{tot} = 10^5$ per cell. (c) Modified Figure 1 from Magro and Alexander (Magro & Alexander, 1974). Plot of histamine release due to 5×10^{-10} M anti-IgE (A) and 5×10^{-8} M (B) incubated with increasing concentrations of monomer anti-IgE (Fab). The insert shows the positioning on the dose response curve of the two anti-IgE concentrations.

activation at $2K_1L = 10^{-4}$ remains practically unaltered, whereas the Syk activation at $2K_1L = 10^4$ increases and approaches the extent of Syk activation at $2K_1L = 10^{-4}$ (Fig. 5b). On the other hand, if the ligand-IgE dissociation constant is increased from 0.3 to 10^3 s^{-1}, the Syk activation at $2K_1L = 10^4$ remains unchanged and that at $2K_1L = 10^{-4}$ decreases and approaches the Syk activation level at $2K_1L = 10^4$ for $k_{-1} = 0.3$ s^{-1} (Fig. 5c). In order to determine the source of asymmetry in the Syk activation curve, we consider a pair of reduced models, which are discussed in the following section.

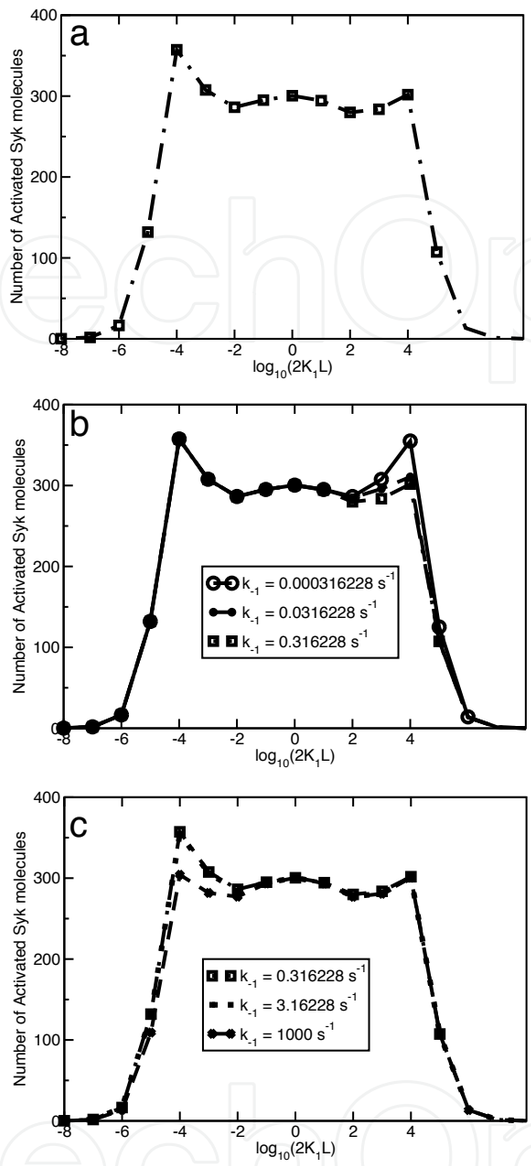

Fig. 5. (a) Syk Activation curve for $k_{+1} = 2.5 \times 10^7$ M^{-1} s^{-1}; $k_{+2} = 8 \times 10^{-9}$cm^{2}s^{-1}; $k_{-1} = 0.316(10^{-0.5})$ s^{-1}; $k_{-2} = 0.0316(10^{-1.5})$s^{-1}; (b)-(c) Syk Activation curves for $k_{+2} = 8 \times 10^{-9}$cm^{2}s^{-1}; $k_{-2} = 0.0316(10^{-1.5})$s^{-1}; (b)The k_{+1} and k_{-1} values are varied such that $K_1 = k_{+1}/k_{-1}$ is fixed at 7.9 $\times 10^7$ M^{-1}. The legends show the k_{-1} values used and the k_{+1} values are accordingly adjusted so that K_1 remains fixed. For parts (a), (b) and (c), $[\text{Syk}]_{tot} = 7 \times 10^3$ per cell; $[\text{Lyn}]_{tot} = 10^5$ per cell; $[\text{Fc}\epsilon\text{RI}]_{tot} = 10^5$ per cell.

3.4 Reduced models of Syk binding to cross-linked receptors

We consider two reduced models, 1 and 2, where the kinetic effects involving Lyn and the β subunit of the receptor have been eliminated. Both models correspond to the limit where the available Lyn is in large excess. In model 1, cross-linked receptors transphosphorylate each other on the γ subunit with a transphosphorylation rate that is the same as that of

Parameter	Description	Value(s)
k_{+1}	ligand-receptor binding forward rate constant	$2.5 \times 10^7 \mathrm{M}^{-1}\mathrm{s}^{-1}$
k_{-1}	ligand-receptor binding reverse rate constant	$0.316(10^{-0.5})\mathrm{s}^{-1}$
k_{+2}	ligand-receptor cross-linking forward rate constant	8.0×10^{-9} $\mathrm{cm}^2\mathrm{mole}^{-1}\mathrm{s}^{-1}$
k_{-2}	ligand-receptor cross-linking reverse rate constant	$0.0316(10^{-1.5})\mathrm{s}^{-1}$

Table 1. Ligand-receptor binding parameters which accentuate the asymmetry in the Syk activation curves. Other rate constants used in our calculations are taken from Faeder et al. (2003). The bimolecular rate constants k_{+1} and k_{+2} are divided by the inverse cell density (1.0×10^{-6} ml) and the cell surface area (8.0×10^{-6} cm^2) to convert them to unimolecular rate constants.

Lyn bound through it SH2 domain to the phosphorylated β subunit of the receptor. As in the full model, bound Syk protects the γ subunit from being dephosphorylated. The rate of dephosphorylation of unprotected phosphorylated γ subunits is the same as in the full model. As seen in Fig. 6a, model 1 exhibits an asymmetry in a plot of Syk dimer formation as a function of the log of the ligand concentration.

In model 2, in addition to assuming Lyn is in excess, all receptor γ subunits are always phosphorylated, thereby eliminating the kinetic effects of receptor phosphorylation. This corresponds to the additional limit that the rate of receptor dephosphorylation goes to zero. For example, if in the full model, the available Lyn is increased from 10^5 to 10^8 per cell and the rate constant for dephosphorylation reduced from 20 s^{-1} to 10^{-4} s^{-1}, then a plot of Syk dimer formation for the full model and model 2 are identical (Fig. 6b). When this second assumption is made, the asymmetry in the Syk dimer curve is eliminated, indicating that the kinetics of phosphorylation and dephosphorylation of the γ subunit plays a role in creating the asymmetry.

3.5 The asymmetry in Syk activation originates from asymmetry in Syk dimer formation.

Since model 1 captures the asymmetry in Syk activation predicted by the full model, we use it to analyze the source of asymmetry in Syk dimer formation. As shown in Fig. 7b for model 1, one can form a Syk dimer (d_0) in a number ways. We have obtained expressions for the mean time required by any particular Syk molecule to end up in a Syk dimer, starting as either cytosolic Syk or as part of a complex with other molecule(s).

3.5.1 Mean time for a Syk molecule to enter into a Syk dimer

We calculate for reduced model 1, the mean times taken by a particular (tagged) Syk molecule to end up in a Syk dimer (Syk-FcϵRI-Ligand-FcϵRI-Syk) starting as either free Syk or as part of a Syk containing complex other than the Syk dimer. In Fig. 7a, we assign notations to different Syk containing species in the reduced model. The mean time taken to form a Syk dimer from species i is given by τ_i. The kinetic parameters used are described in Table 2. We define the mean time of incorporation of the tagged Syk molecule in species d_0, starting from species i, in the following fashion. This mean time is divided into two parts, the first part corresponding to the mean time of transition from species i to all other species containing the tagged Syk molecule. This is the inverse of the sum of rates of all processes that transform species i to the

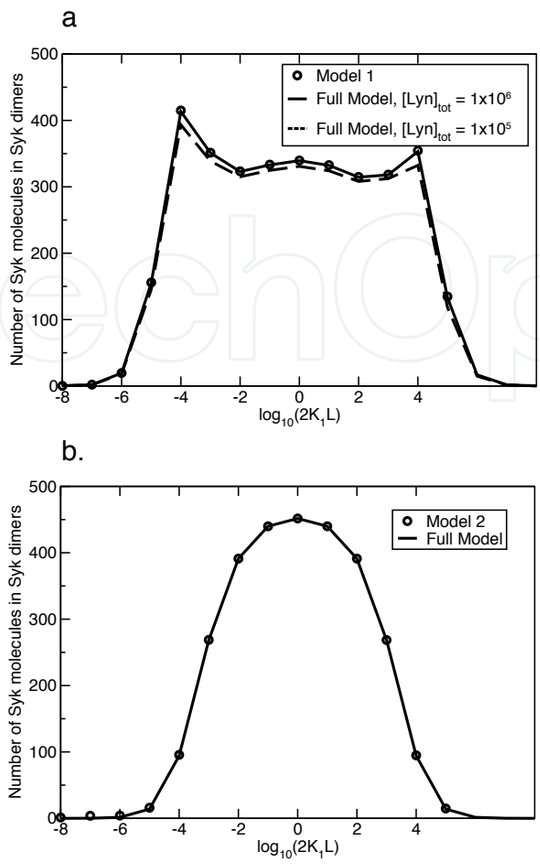

Fig. 6. Comparison of number of Syk dimers per cell obtained using reduced model 1 and 2, with the corresponding numbers obtained using the full model. $[\text{Syk}]_{tot} = 7 \times 10^3$ per cell; $[\text{Fc}\epsilon\text{RI}]_{tot} = 10^5$ per cell. We use the same ligand-receptor and Syk-pγ binding and unbinding parameters as in Table 2 for both the reduced models and the full model. (a) We consider two different total cellular concentrations of Lyn in the full model, $[\text{Lyn}]_{tot} = 10^5$ and $[\text{Lyn}]_{tot} = 10^6$ per cell. (b) Comparison of reduced model 2 to the full model when Lyn is in large excess and the rate of dephosphorylation is negligible ($[\text{Lyn}]_{tot} = 10^8$ per cell, $k_{-p} = 10^{-4}\text{s}^{-1}$).

other species. The second part represents the mean remaining time to incorporate the tagged Syk in the Syk dimer species d_0. In terms of the species from Fig. 7a and the kinetic parameters from Table 2, the mean times of transition from species a_0, b_0, c_0, c_1 and s_0 respectively.

$$m_{a0} = \frac{1}{k_{+2}(b_0 + b_1 + b_2) + k_{-1} + k_{-S}} \tag{1}$$

$$m_{b0} = \frac{1}{k_{+2}(a_0 + a_1 + a_2) + 2k_{+1}L + k_{-S}} \tag{2}$$

$$m_{c0} = \frac{1}{2k_{-2} + k_{-S} + k_{-p} + k_{+S}s_0} \tag{3}$$

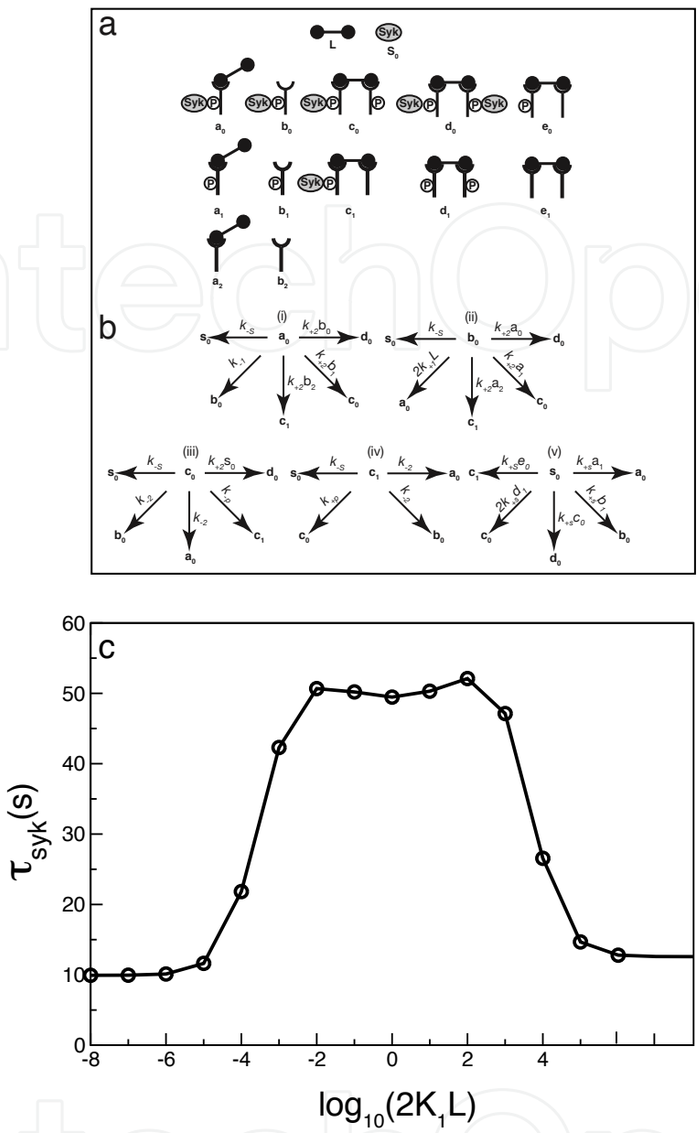

Fig. 7. (a) Schematic representation of the different Syk containing species in the reduced model 1. We tag a particular Syk molecule and calculate the mean time required by this Syk molecule to be incorporated into a Syk dimer (d_0). (b) (i-v) shows the different routes by which a tagged Syk molecule can be transferred from one species to another. (c) Mean time τ_{Syk} taken by any particular Syk molecule to be incorporated into a Syk dimer, starting as cytosolic Syk (s_0) or as other specie(s) (a_0, b_0, c_0, c_1) in (a). The rate parameters are taken from Table. 2. $[\text{Syk}]_{tot} = 7 \times 10^3$ per cell; $[\text{Fc}\epsilon\text{RI}]_{tot} = 10^5$ per cell.

$$m_{c1} = \frac{1}{2k_{-2} + k_{-S} + k_{+p}} \tag{4}$$

$$m_{s0} = \frac{1}{k_{+S}(a_1 + b_1 + 2d_1 + c_0 + e_0)} \tag{5}$$

Parameter	Description	Value(s)
k_{+1}	ligand-receptor binding forward rate constant	$2.5 \times 10^7 \mathrm{M}^{-1}\mathrm{s}^{-1}$
k_{-1}	ligand-receptor binding reverse rate constant	$0.316(10^{-0.5})\mathrm{s}^{-1}$
k_{+2}	ligand-receptor cross-linking forward rate constant	8.0×10^{-9} $\mathrm{cm}^2\mathrm{mole}^{-1}\mathrm{s}^{-1}$
k_{-2}	ligand-receptor cross-linking reverse rate constant	$0.0316(10^{-1.5})\mathrm{s}^{-1}$
k_{+gP}	receptor γ phosphorylation forward rate constant	$3.0\ \mathrm{s}^{-1}$
k_{-gP}	receptor γ dephosphorylation rate constant	$20\mathrm{s}^{-1}$
k_{+S}	Syk-phosphorylated receptor γ binding forward rate constant	6.0×10^{-5} $\mathrm{molecule}^{-1}\mathrm{s}^{-1}$
k_{-S}	Syk-phosphorylated receptor γ reverse rate constant	$0.13\mathrm{s}^{-1}$

Table 2. Kinetic parameters used in reduced model with receptor γ phosphorylation-dephosphorylation. The bimolecular rate constants are divided by the inverse cell density (1.0×10^{-6} ml) and the cell surface area (8.0×10^{-6} cm^2) to convert them to unimolecular rate constants.

In terms of the above quantitites, τ_i can be defined as follows.

$$\tau_{a0} = m_{a0}[1 + (k_{+2}b_1\tau_{c0} + k_{+2}b_2\tau_{c1} + k_{-1}\tau_{b0} + k_{-S}\tau_{s0})] \tag{6}$$

$$\tau_{b0} = m_{b0}[1 + (k_{+2}a_1\tau_{c0} + k_{+2}a_2\tau_{c1} + 2k_{+1}L\tau_{a0} + k_{-S}\tau_{s0})] \tag{7}$$

$$\tau_{c0} = m_{c0}[1 + (k_{-2}\tau_{a0} + k_{-2}\tau_{b0} + k_{-S}\tau_{s0} + k_{-p}\tau_{c1})] \tag{8}$$

$$\tau_{c1} = m_{c1}[1 + (k_{-2}\tau_{a0} + k_{-2}\tau_{b0} + k_{-S}\tau_{s0} + k_{+p}\tau_{c0})] \tag{9}$$

$$\tau_{s0} = m_{s0}[1 + (k_{+S}a_1\tau_{a0} + k_{+S}b_1\tau_{b0} + 2k_{+S}d_1\tau_{c0} + k_{+S}e_0\tau_{c1})] \tag{10}$$

The above equations are solved for τ_{a0}, τ_{b0}, τ_{c0}, τ_{c1} and τ_{s0} using parameters from Table 2 for different L values corresponding to $\log_{10}(2K_1L)$ values from -8 to 8. The expression levels of Syk and FcϵRI receptor per cell are taken as 7×10^3 and 10^5 respectively. The mean time for any tagged Syk molecule to be incorporated into a Syk dimer (d_0) is given by

$$\tau_{Syk} = p_{a0}\tau_{a0} + p_{b0}\tau_{b0} + p_{c0}\tau_{c0} + p_{c1}\tau_{c1} + p_{s0}\tau_{s0} \tag{11}$$

where

$$\begin{aligned} &p_{a0} = a_0/[\mathrm{Syk}]_{tot};\ p_{b0} = b_0/[\mathrm{Syk}]_{tot};\ p_{c0} = c_0/[\mathrm{Syk}]_{tot};\\ &p_{c1} = c_1/[\mathrm{Syk}]_{tot};\ \ p_{s0} = s_0/[\mathrm{Syk}]_{tot} \end{aligned} \tag{12}$$

and $[\mathrm{Syk}]_{tot} = a_0 + b_0 + c_0 + c_1 + 2d_0 + s_0$. The quantity τ_{Syk} is plotted as a function of $\log_{10}2K_1L$ in Fig. 7c. This mean time τ_{Syk} is not symmetric with respect to reflection about $2K_1L = 1$. The mean time at $2K_1L = 10^{-4}$ is less than its counterpart at $2K_1L = 10^4$, as shown in Fig 7c.

3.6 The asymmetry in Syk activation depends on the receptor-ligand dissociation constant

In Fig. 8a, we vary k_{-1} and k_{+1} keeping their ratio K_1 fixed, and calculate the average time τ_{Syk} required by a Syk to end up in a Syk dimer. At $k_{-1} = 10^{-3.5}$ s^{-1}, the τ_{Syk} values at $2K_1L = 10^{-4}$ and $2K_1L = 10^4$ are close to each other, so that there is little difference in the extent of Syk activation at these two ligand concentrations as was seen in Fig. 5b. As k_{-1} is increased from $10^{-3.5}$ s^{-1}, τ_{Syk} at $2K_1L = 10^{-4}$ remains unchanged while τ_{Syk} at $2K_1L = 10^4$ increases. This is consistent with our results from the full model, that Syk activation at

$2K_1L = 10^{-4}$ is essentially unchanged, while Syk activation at $2K_1L = 10^4$ decreases as k_{-1} is increased and K_1 is kept fixed (Fig. 5b). The difference between the τ_{Syk} values at the two ligand concentrations increases, as does the asymmetry in Syk activation obtained using the full model. When k_{-1} is increased beyond 0.316 ($10^{-0.5}$) s^{-1}, τ_{Syk} at $2K_1L = 10^{-4}$ increased while τ_{Syk} at $2K_1L = 10^4$ reaches a plateau. As a result, the difference in the τ_{Syk} values at these two ligand concentrations decreases with increasing k_{-1}. As k_{-1} is increased to 10^3 s^{-1}, τ_{Syk} at both $2K_1L = 10^{-4}$ and $2K_1L = 10^4$ approaches the same value. This is the same trend exhibited by Syk activation in the full model (Fig. 5c). The strong correlation between τ_{Syk} from reduced model 1 and Syk activation in the full model supports the idea that the asymmetry in the Syk activation profile originates from the asymmetry in τ_{Syk}.

The question remains, how can the kinetics of ligand binding, which occurs on the outside of the cell, give rise to an asymmetry in the Syk activation curve, when the receptor cross-linking curve is symmetric? To answer the question we considered two receptors, one free and one bound. These receptors might, for example, have come from a receptor dimer when it dissociated and their cytoplasmic domains may be associated with Syk or Lyn or both. We show how to calculate two quantities at equilibrium, τ_R and τ_B, the mean times respectively of an unbound receptor to enter into an aggregate and for a bound receptor that is not cross-linked to a second receptor to enter into an aggregate (Fig. 9a).

3.6.1 Mean time for a receptor to enter into a receptor dimer

We consider the case the cross-linking of monovalent receptors by a bivalent ligand. There are two possible transitions an unbound receptor can undergo. It can interact with a bound receptor to form a dimer or it can bind to a ligand in solution to become a bound receptor. Similarly two transitions are possible for a bound receptor that is not in an aggregate. It can associate with a free receptor to form a dimer or it can detach from its ligand and become a free receptor. These transitions are illustrated in Fig. 9a where the rates of transition are given.

The mean times τ_R and τ_B will be found by solving two linear algebraic equations that are functions of the equilibrium concentrations of the free receptors, R, and the bound receptors not in dimers, B. At equilibrium, these concentrations are calculated from the single site equilibrium constants for binding and crosslinking, K_1 and K_2 respectively, and the total receptor and ligand concentrations, R_T and L_T. However, for our purposes, it is more useful to express the results in terms of the free ligand concentration.

If there are R_T total receptors on the cell surface and there are no processes that remove or add new receptors the the total number of receptors is conserved and

$$\begin{aligned} R_T &= R + B + 2D = R + 2K_1LR + 2(2K_1L)(K_2/2)R^2 \\ &= (1 + 2K_1L)R + 2K_1K_2LR^2 \end{aligned} \tag{13}$$

where D is the concentration of receptor dimers. Defining $r = R/R_T$ as the fraction of free receptors Eq. (13) becomes

$$1 = (1 + 2K_1L)r + 2K_1K_2R_TLr^2 \tag{14}$$

It can be shown that w, the fraction of receptors not in dimers is given by

$$w = (1 + 2K_1L)r = \frac{-1 + \sqrt{1 + 4\delta}}{2\delta} \tag{15}$$

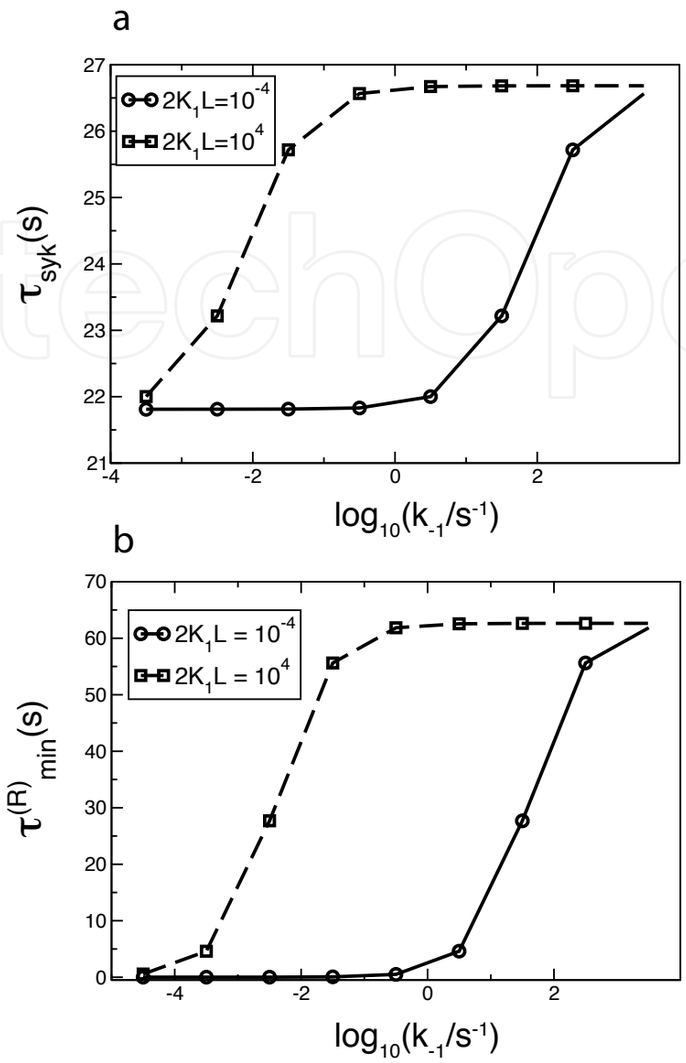

Fig. 8. Variation with k_{-1} of (a) average time (τ_{Syk}) required by any particular Syk molecule to end up in a Syk dimer and (b) minimum time ($\tau_{min}^{(R)}$) required by a receptor to be incorporated into a receptor dimer, at ligand concentrations given by $2K_1L = 10^{-4}$ and $2K_1L = 10^4$. The k_{-1} and k_{+1} are varied in such a way that $K_1 = k_{+1}/k_{-1}$ remains fixed at 7.9×10^7 M^{-1}. Other rate constants are taken from Table 2. $[Syk]_{tot} = 7 \times 10^3$ per cell; $[Fc\epsilon RI]_{tot} = 10^5$ per cell.

where

$$\delta = \frac{2K_1K_2R_TL}{(1+2K_1L)^2} \tag{16}$$

It follows that

$$R = wR_T\frac{1}{1+2K_1L} \tag{17}$$

$$B = wR_T\frac{2K_1L}{1+2K_1L} \tag{18}$$

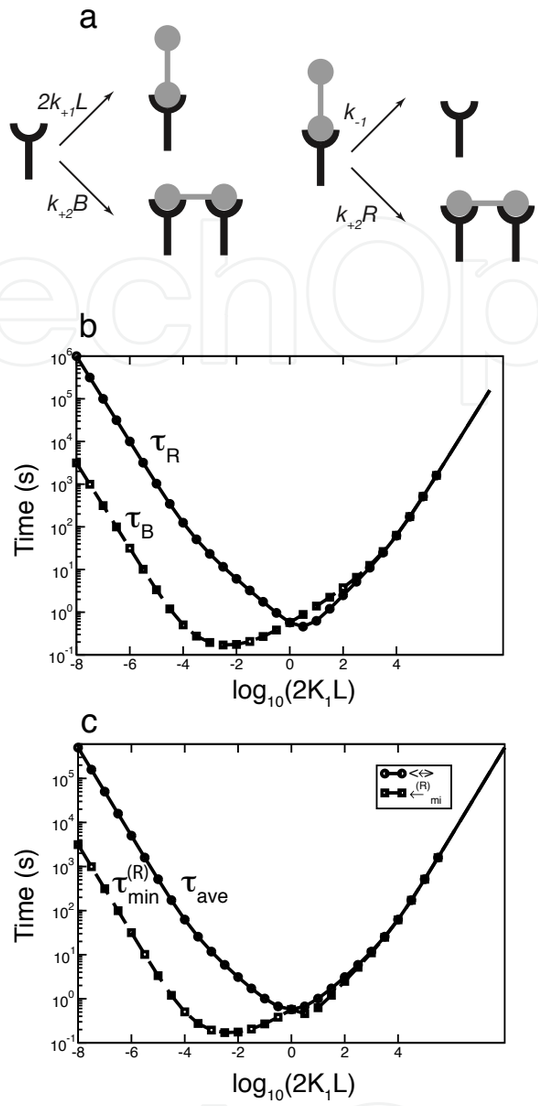

Fig. 9. (a) Rate constants that characterize the transitions that a free receptor and a bound receptor not in an aggregate can undergo. (b) The mean times for a free receptor (τ_R) and a bound receptor (τ_B) to find a partner and form a dimer as functions of the bivalent ligand concentration. (c) The mean τ_{ave} of τ_R and τ_B and the minimum $\tau_{min}^{(R)}$ of τ_R and τ_B as a function of the ligand concentration. In parts (b) and (c), the ligand receptor binding and cross-linking parameters are taken from Table 2 and $[\text{Fc}\epsilon\text{RI}]_{tot} = 10^5$ per cell.

We next write down the equations for the mean times.

$$\tau_B = \frac{1}{k_{+2}R + k_{-1}} + \frac{k_{-1}}{k_{+2}R + k_{-1}}\tau_R \tag{19}$$

$$\tau_R = \frac{1}{k_{+2}B + 2k_{+1}L} + \frac{2k_{+1}L}{k_{+2}B + 2k_{+1}L}\tau_B \tag{20}$$

The first term in each equation is the mean time to make a transition, while the second term is the mean remaining time after the first transition until the receptor is incorporated into a dimer. We define the following quantities:

$$t_1 = \frac{1}{k_{+2}R + k_{-1}} \qquad t_2 = \frac{1}{k_{+2}B + 2k_{+1}L} \tag{21}$$

$$p_1 = \frac{k_{-1}}{k_{+2}R + k_{-1}} \qquad p_2 = \frac{2k_{+1}L}{k_{+2}B + 2k_{+1}L} \tag{22}$$

The ts are mean times to make a transition while the ps are probabilities of making specific transitions.

Eqs. (19) and (20) hold whether or not the system is in equilibrium. At equilibrium, there are simplifications. For example, at equilibrium, $p_1 = p_2$, i.e., the probability of a ligand dissociating from a bound receptor is equal to the probability of a free receptor binding a ligand. This must be so if equilibrium is to be maintained. Solving Eqs. (19) and (20), we have

$$\tau_B = \frac{t_1 + p_1 t_2}{1 - p_1 p_2} \tag{23}$$

$$\tau_R = \frac{t_2 + p_2 t_1}{1 - p_1 p_2} \tag{24}$$

3.6.2 Asymmetry in Syk activation profile results from differential minimum time for a receptor to reform a dimer at different ligand concentrations

In Fig. 9b we show the mean times τ_R and τ_B as functions of the bivalent ligand concentration. Neither are symmetric, nor is their minimum, although their sum is symmetric (Fig.9c). Monovalent binding is responsible for the asymmetry. Consider the mean times at two free ligand concentrations, L_+ and L_-, where $\log(2K_1L_+) = -\log(2K_1L_-)$. At L_-, the bound receptor gets incorporated into a dimer more rapidly than the unbound receptor because it is present in the lowest concentration, and so it more rapidly finds a partner to crosslink. At L_+ the opposite is true. The asymmetry that arises in the minimum time for a receptor to reform a dimer, $\tau_{min}^{(R)}$, results from an asymmetric effect of the free ligand concentration on the lifetime of the minority receptor (the receptor at lowest concentration). At high ligand concentrations, minority receptors (unbound) are rapidly converted to bound receptors giving them less time to enter into a dimer. Thus, they may have to undergo interconversion between unbound and bound forms many times before forming a dimer. At low ligand concentrations, the initial conversion of the minority receptors (bound) to the unbound form is independent of the ligand concentration, depending only on the rate of dissociation.

In Fig. 8b we keep the equilibrium constant $K_1 = k_{+1}/k_{-1}$ fixed and, for the same set of parameters as in Fig. 8a, vary k_{-1}. We observe that the dependence of $\tau_{min}^{(R)}$ on $\log_{10}(k_{-1}/s^{-1})$ at the two ligand concentrations given by $2K_1L = 10^{-4}$ and $2K_1L = 10^4$ is qualitatively similar to that of τ_{Syk}. Since receptor dimerization is upstream from, and necessary for Syk activation, we infer that the dependence of τ_{Syk} on k_{-1} results from the corresponding dependence of $\tau_{min}^{(R)}$ on k_{-1}.

4. Serial engagement of IgE-FcϵRI complexes can enhance Syk activation in mast cells

As we have mentioned earlier in this chapter, mast cell responses mediated by FcϵRI are initiated when a multivalent ligand, an allergen for example, aggregates the receptors. In order to maintain the cellular response, it is not required that new aggregates constantly form. Kent et al. (Kent et al., 1994) exposed RBL cells to covalently cross-linked oligomers of IgE for a short duration and then added excess monomeric IgE to prevent further aggregation of receptors. Under these conditions, aggregated receptors continued to propagate the cellular signal. Phosphorylation of the β and γ immunoreceptor tyrosine-based activating motifs (ITAMs), phosphorylation of the protein tyrosine kinase Syk, and the release of histamine containing granules were sustained for substantial lengths of time after new aggregate formation was blocked. Although serial engagement of IgE-FcϵRI complexes is not necessary for mast cell signaling, the question still remains whether serial engagement can enhance mast cell response at low allergen concentrations. After deriving an expression for the rate at which a ligand of valence N serially engages receptors on a surface, we have refined this question and used the model of Faeder et al. (2003) to answer it.

4.1 Extension of mathematical model to simulate Syk activation in RBL cells stimulated by trivalent ligands

Earlier in this chapter, we have discussed how the model of Faeder et al. (2003) has been used to simulate the early response of RBL cells to the addition of a reversible bivalent ligand that binds to, and dimerizes, IgE-Fc complexes on RBL cell surfaces. The model consists of a network of 354 distinct chemical species connected by 3680 chemical reactions, 21 rate constants and three concentrations, the surface concentrations of FcϵRI and available Lyn, and the total concentration of Syk. With the exception of the rate constants that describe the interaction of the bivalent ligand with IgE, k_{+1}, k_{-1}, k_{+2} and k_{-2}, the parameters used in the simulations are the same as those given in Table I of Faeder et al. (2003). In the simulations for the current investigation, we take $k_{\text{off}} = k_{-1} = k_{-2}$ and the total concentrations of Lyn, Syk and FcϵRI are specific for RBL cells.

We now generalize our model to simulate the early signaling events triggered by the addition of a symmetric trivalent ligand with three identical binding sites interacting with IgE bound to FcϵRI on RBL cells. There is now an additional surface crosslinking reaction involving a trivalent ligand with two of its sites bond crosslinking a third IgE-FcϵRI, described by rate constants k_{-3} and k_{+3}. In the simulations, we take $k_{\text{off}} = k_{-1} = k_{-2} = k_{-3}$ and $k_{+2} = k_{+3}$. It is assumed that a Lyn bound to a receptor can randomly transphosphorylate any other receptor in the aggregate with the same rates, as it was assumed for the dimeric aggregate. For the trivalent ligand, the model expands to 2954 distinct chemical species connected by 49948 reactions.

4.2 Theory

First, we obtain an expression for the rate of serial engagement of a multivalent ligand of valence N binding to free mobile receptors on a cell surface that has a concentration of R free receptors. This expression allows us to choose parameter values that define ligands with different rates of serial engagement. We then use these parameter values to simulate the early response of mast cells to ligands that serial engage receptors at different rates. We use as our

measure of signaling response, receptors that have fully activated Syk associated with their γ ITAMs. Syk becomes partially active upon binding through its two SH2 domains to the doubly phosphorylated γ ITAM (Shiue et al., 1995). In our model, Syk is fully active when it has been transphosphorylated on its activation loop tyrosines by a second Syk (reviewed in Faeder et al. (2003)). Finally, we use the results of the simulations to evaluate the role of serial engagement in early responses of mast cell signaling.

4.2.1 Serial engagement of a N-valent ligand

The rate of serial engagement equals the number of receptors the ligand encounters from the time t_a it first attaches to a cell surface receptor until the time t_b when its last bond breaks, divided by the time this process lasted, $t_b - t_a$. Figure 10 illustrates the reactions a five valent ligand can undergo once it is initially bound to a receptor on a surface. The mean time an N-valent ligand, that initially has one site bound to a receptor, remains on a surface when the concentration of free receptors is R is (Hlavacek et al., 2002; 1999)

$$t_N = \frac{1}{k_{\text{off}}}\left[\frac{(1+K_2R)^N - 1}{NK_2R}\right] \tag{25}$$

where $K_2 = k_{+2}/k_{\text{off}}$ is the equilibrium cross-linking constant.

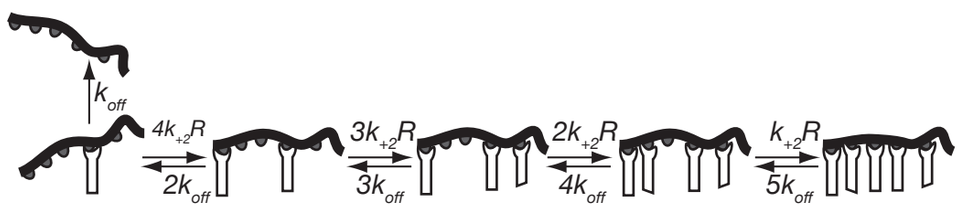

Fig. 10. The multiple reactions a ligand of valence five ($N = 5$) can undergo from the time it first binds a cell surface receptor until the last ligand-receptor bond breaks and the ligand leaves the surface. R is the concentration of free receptors. In these reactions, k_{+2} is the single-site rate constant for addition of a receptor to a ligand-receptor complex and k_{off} is the corresponding reverse rate constant. By taking all the forward and reverse rate constants to be the same, we have assumed that these rate constants are independent of the bound state of the ligand.

In the following section, we derive the following expression for n_N, the mean number of receptors an N-valent ligand that initially has one site bound to a receptor, serial engages before it dissociates from the cell surface.

4.2.2 Average number of receptors serially engaged by a multivalent ligand

An expression for the average number of receptors a multivalent ligand serially engages, n_N, is obtained by solving a set of ordinary differential equations (ODEs). We consider a cell with monovalent receptors on its surface that is in equilibrium with a homogeneous concentration of N-valent ligands. At equilibrium, there is a distribution of bound ligands, some with one site bound, some with two sites bound, up to some with N sites bound. We consider the

ensemble of N-valent ligands that, at $t = 0$, have one and only one site bound to a receptor. We let $B_i(t)$ be the fraction of these ligands that have i sites bound at time t or equivalently, the probability that a ligand has i sites bound at time t when initially it had one site bound. We keep track of the number of receptors a ligand serial engages by keeping track of how many receptors dissociate from a ligand until the ligand leaves the cell surface. Since the rate at which a receptor dissociates from a ligand with i sites bound is ik_{off}, the averaged number of receptors a ligand will serial engage from the time it binds to the cell until the time it leaves the cell is:

$$n_N = k_{\text{off}} \int_0^\infty \Big(2B_2(t') + 3B_3(t') \cdots + NB_N(t')\Big) dt' \tag{26}$$

Before solving the general problem, we illustrate our approach by finding the number of receptors a bivalent ligand serial engages during its time on the cell surface.

The equilibrium concentration of free receptors we call R. For a bivalent ligand, we have the following set of ODEs:

$$\frac{dB_1}{dt} = -k_{\text{off}}B_1 - k_{+2}RB_1 + 2k_{\text{off}}B_2 \tag{27}$$

$$\frac{dB_2}{dt} = k_{+2}RB_1 - 2k_{\text{off}}B_2 \tag{28}$$

The initial conditions are that $B_1 = 1$ and $B_2 = 0$.

The average number of receptors a bivalent ligand engages during its time on the cell surface is

$$n_2 = 2k_{\text{off}} \int_0^\infty B_2(t')dt' \tag{29}$$

As is standard, we use Laplace transforms ($\mathcal{L}$), to transform the problem into solving a set of algebraic equations, taking s to be the transform variable and $\bar{B}_i(s) = \mathcal{L}[B_i(t)]$. Note that

$$n_N = \lim_{s\to 0} k_{\text{off}} \Big(2\bar{B}_2(s) + 3\bar{B}_3(s) \cdots + N\bar{B}_N(s)\Big) \tag{30}$$

This follows because the Laplace transform of $\int_0^t f(u)du$ is $\bar{f}(s)/s$ and

$$\lim_{t\to\infty} g(t) = \lim_{s\to 0} s\bar{g}(s) \tag{31}$$

Taking Laplace transforms of both sides of Eqs. (27) and (28), we have

$$s\bar{B}_1 - B_1(0) = -k_{\text{off}}\bar{B}_1 - k_{+2}R\bar{B}_1 + 2k_{\text{off}}\bar{B}_2$$
$$sB_2 = k_{+2}R\bar{B}_1 - 2k_{\text{off}}\bar{B}_2$$

We can take the limit before we solve the equations. Setting $s = 0$, $k = k_{+2}R/k_{\text{off}} = K_2R$ and $B_1(0) = 1$,

$$\frac{1}{k_{\text{off}}} = (1+k)\bar{B}_1 - 2\bar{B}_2$$
$$0 = k\bar{B}_1 - 2\bar{B}_2$$

Solving, we have that $B_2 = k/(2k_{\text{off}})$ and

$$n_2 = \lim_{s\to 0} k_{\text{off}} 2B_2(s) = k = K_2R \tag{32}$$

For a ligand with valence N,

$$\frac{dB_i}{dt} = (i+1)k_{\text{off}}B_{i+1} + (N-i+1)k_{+2}RB_{i-1} - ik_{\text{off}}B_i - (N-i)k_{+2}RB_i \tag{33}$$

B_i can appear through dissociation of a receptor from any of $i+1$ receptor-occupied sites of B_{i+1}, which corresponds to a term $(i+1)k_{\text{off}}B_{i+1}$, and through engaging of a receptor by any of $(N-(i-1))$ free sites of B_{i-1}, which corresponds to a term $(N-i+1)k_{+2}RB_{i-1}$. B_i can disappear by losing a receptor from any of its i receptor-bound sites and by adding a receptor to any of $(N-i)$ free sites, which corresponds to substraction of terms $ik_{\text{off}}B_i$ and $(N-i)k_{+2}RB_i$ respectively.

Putting $k = k_{+2}R/k_{\text{off}}$, $\tau = k_{\text{off}}t$, $B_0 = B_{N+1} = 0$, and collecting terms,

$$\frac{dB_i}{d\tau} = (i+1)B_{i+1} - (i+k(N-i))B_i + k(N-i+1)B_{i-1},\ i = 1,\ldots,N \tag{34}$$

(Note that $B_0 = B_{N+1} = 0$ implies that the corresponding Laplace transforms $\bar{B}_0 = \bar{B}_{N+1} = 0$.)

As before, taking Laplace transforms and setting the transform variable equal to zero, we obtain

$$\begin{aligned}
-1 &= 2\bar{B}_2 - (1+k(N-1))\bar{B}_1 \\
0 &= 3\bar{B}_3 - (2+k(N-2))\bar{B}_2 + (N-1)k\bar{B}_1 \\
0 &= 4\bar{B}_4 - (3+k(N-3))\bar{B}_3 + (N-2)k\bar{B}_2 \\
&\vdots \\
0 &= -N\bar{B}_N + k\bar{B}_{N-1}
\end{aligned}$$

First, we solve this system of equations for $\bar{B}_1$ by summing all the equations:

$$\begin{aligned}
-1 &= \sum_{i=1}^{N}\left((i+1)\bar{B}_{i+1} - (i+k(N-i))\bar{B}_i + k(N-i+1)\bar{B}_{i-1}\right) \\
&= \sum_{i=2}^{N} i\bar{B}_i - \sum_{i=1}^{N}(i+k(N-i))\bar{B}_i + \sum_{i=1}^{N-1} k(N-i)\bar{B}_i \\
&= \sum_{i=1}^{N}\left(i - (i+k(N-i)) + k(N-i)\right)\bar{B}_i - \bar{B}_1
\end{aligned}$$

Each term in the sum on the right hand side equals zero, so that $\bar{B}_1 = 1$. To find $\bar{B}_2$, we sum up all equations except the first one:

$$\begin{aligned}
0 &= \sum_{i=2}^{N}\left((i+1)\bar{B}_{i+1} - (i+k(N-i))\bar{B}_i + k(N-i+1)\bar{B}_{i-1}\right) \\
&= \sum_{i=3}^{N} i\bar{B}_i - \sum_{i=2}^{N}(i+k(N-i))\bar{B}_i + \sum_{i=1}^{N-1} k(N-i)\bar{B}_i \\
&= \sum_{i=2}^{N}\left(i - (i+k(N-i)) + k(N-i)\right)\bar{B}_i - 2\bar{B}_2 + k(N-1)\bar{B}_1
\end{aligned}$$

	$K_2R = 0.1$			$K_2R = 1.0$			$K_2R = 10.0$		
N	$k_{off}t_N$	n_N	$r_N k_{off}^{-1}$	$k_{off}t_N$	n_N	$r_N k_{off}^{-1}$	$k_{off}t_N$	n_N	$r_N k_{off}^{-1}$
2	1.05	0.10	0.095	1.50	1.00	0.67	6.00	10.00	1.67
3	1.10	0.21	0.190	2.33	3.00	1.29	44.33	120.00	2.71
4	1.16	0.33	0.285	3.75	7.00	1.87	366.00	1330.00	3.63
5	1.22	0.46	0.380	6.20	15.00	2.42	3221.00	14640.00	4.55

Table 3. The influence of the parameter K_2R (the product of the equilibrium cross-linking constant and the free receptor concentration) on the mean time a N-valent ligand remains bound to the surface (t_N), the mean number of receptors the ligand engages while it remains bound to the surface (n_N), and the rate the ligand serial engages receptors (r_N). Increasing K_2R increases the rate at which a ligand cross-links a receptor compared to the rate at which a receptor dissociates from the ligand.

Again, the first sum on the right hand side equals zero so that $\bar{B}_2 = k(N-1)\bar{B}_1/2 = k(N-1)/2$. Similarly, $\bar{B}_3 = k(N-2)\bar{B}_2/3 = k^2(N-1)(N-2)/(1\cdot 2\cdot 3)$. Following this approach, it is straightforward to show that

$$\bar{B}_j = k^{j-1}\frac{(N-j+1)(N-j+2)\ldots(N-1)}{j!} = k^{j-1}\frac{(N-1)!}{j!(N-j)!} \tag{35}$$

and therefore, that

$$n_N = \sum_{j=2}^{N} j\bar{B}_j = \sum_{j=2}^{N} k^{j-1}\frac{(N-1)!}{(j-1)!(N-j)!} \tag{36}$$

4.2.3 Average rate of serial engagement

The average rate, r_N, an N-valent ligand serially engages receptors is

$$r_N = n_N/t_N \tag{37}$$

In Table 3 we evaluate these expressions for $N = 1-5$ and $K_2R = 0.10, 1.0$ and 10.0. The parameter K_2R is the product of the surface equilibrium cross-linking constant and the surface concentration of free receptors. Larger values of K_2R favor aggregate formation. Note that for large values of K_2R, as the valence is increased, the number of serial engagements and the mean time the ligand remains bound to the cell rises rapidly but their ratio, the rate of serial engagement, increases only modestly. From Eqs (25)-(37) it can be shown that the maximal rate of serial engagement achievable by an N-valent ligand when k_{off} is fixed and $k_{+2}R$ is increased is Nk_{off}. When $k_{+2}R$ is fixed and k_{off} is increased, the maximal rate is $k_{+2}R$.

4.2.4 The rates of serial engagement of receptors for bivalent and trivalent ligands

We now focus on bivalent and trivalent ligands interacting with monovalent receptors. From Eqs. (25) - (37) we have that the rate of serial engagement of a bivalent ligand

$$r_2 = 2k_{off}\frac{K_2R}{2+K_2R} \tag{38}$$

A second way this result can be obtained is to note that one receptor is bound and released by a bivalent ligand in one cycle time t_c so that $r_2 = 1/t_c$. The cycle time is the sum of the

mean times for a site on a doubly bound ligand to open and for the singly bound ligand to bind to another receptor, i.e., $t_c = 1/(2k_{\text{off}}) + 1/(k_{+2}R)$. (When the ligand is a pMHC rather than a bivalent ligand the two in Eq. (38) becomes a one (Wofsy et al., 2001).) This simple approach for calculating r_2 cannot easily be generalized to ligands with valence greater than two because for these ligands, there is more than one recycling time.

From Eqs. (25) - (37), we have the rate of serial engagement of a trivalent ligand

$$r_3 = 3k_{\text{off}} \frac{2K_2R + (K_2R)^2}{3 + 3K_2R + (K_2R)^2} \tag{39}$$

It is easy to see from these expressions that for large values of K_2R, the rate of serial engagement approaches its maximal value of Nk_{off}. We use Eqs. (38) and (39) to pick the parameter values that characterize the ligands for our simulations.

There are three separate ways to vary the ligand properties to enhance serial engagement, increase k_{off}, increase k_{+2} or increase the valence of the ligand:

1. Increasing k_{off} enhances the rate at which the ligand serial engages receptors but this has the deleterious effect of enhancing kinetic proofreading by reducing the time a receptor remains in an aggregate. Once a receptor leaves an aggregate, unless it can rapidly enter into a new aggregate, all modifications it has undergone will be reversed and it will return to its basal state (Mao & Metzger, 1997; Peirce & Metzger, 2000).

2. Increasing k_{+2} reduces the time it takes a free site on a ligand in a ligand-receptor complex to bind to a new receptor. This enhances the effects of serial engagement by making it more likely that a ligand-receptor complex will form a new dimer before the ligand dissociates and the receptor returns to its basal state.

3. Increasing the valence of the ligand has a similar effect to increasing the forward rate constant. For an N-valent ligand bound through a single site to a receptor, the forward rate of binding a second receptor and forming a dimer is proportional to $(N-1)k_{+2}$. However, increasing the valence introduces other effects as well. A higher valent ligand can form larger aggregates and large aggregates are more effective at signaling than smaller aggregates, even when the ligands are oligomers of IgE that do not undergo serial engagement (Fewtrell & Metzger, 1980). In RBL cells, Lyn, the kinase that is responsible for ITAM phosphorylation, is limiting (Torigoe et al., 1997; Wofsy et al., 1997). Therefore, larger aggregates have a higher probability than receptor dimers of containing a receptor associated with Lyn, and a Lyn in an aggregate can serial phosphorylate all its neighboring receptors in the aggregate.

4.3 Simulations of mast cell responses to bivalent and trivalent ligands for different rates of serial engagement

We use our model to assess the role of serial engagement in mast cell signaling. The predicted outputs of the model that we use in our study are the concentrations (number per cell) of the phosphorylated β and γ ITAMs of FcϵRI, and the concentration of Syk bound to a phosphorylated γ ITAM and transphosphorylated on its activation loop tyrosines by a Syk bound to an adjacent receptor. We refer to Syk bound to the γ ITAM and phosphorylated on its activation loop tyrosines as fully activated Syk or phosphorylated Syk. Using antibodies specific for phosphorylated tyrosines in the activation loop of Syk, it has been shown that upon FcϵRI aggregation, these tyrosines became phosphorylated and this phosphorylation

depended on the kinase activity of Syk (Zhang et al., 2000). The presence of these activation loop tyrosines are necessary for Syk-mediated propagation of FcϵRI signaling (Zhang et al., 1998).

4.3.1 Increasing serial engagement by increasing k_{off} reduces Syk activation

In Figure 11 we compare the predicted levels of β and γ ITAM phosphorylation and full Syk activation induced by four different hypothetical ligands, two bivalent (circles) and two trivalent (squares), that have the same single site forward rate constants $k_{+2} = 2.0 \times 10^{-11}$ cm^2/s. (In the simulations, we take the surface area of the cell $A = 8 \times 10^{-6}$ cm^2 and the total number of receptors per cell $N_T = 4 \times 10^5$ so that the receptor density $R_T = 5 \times 10^{10}$ cm^{-2}. Therefore, at low ligand concentrations, when most of the receptors are free so that $R \approx R_T$, the rate at which a bound ligand with one site free cross-links a receptor is $k_{+2}R = 1.0$ s^{-1}.) Each pair of bivalent and trivalent ligands have dissociation rate constants $k_{\text{off}} = 0.01$ s^{-1} (solid lines and symbols) and 10 s^{-1} (dashed lines and open symbols). For the dimer, increasing k_{off} from 0.01 s^{-1} to 10 s^{-1} corresponds to increasing the rate of serial engagement from $r_2 = 0.017$ s^{-1} to 0.10 s^{-1} (Eq. 38), while for the trimer, the increase is from $r_3 = 0.027$ s^{-1} to 0.20 s^{-1} (Eq. 39). In addition to increasing the rate of serial engagement, increasing k_{off} reduces the lifetime of the bond between a site on the ligand and a receptor site and thus, increases the effects of kinetic proofreading (McKeithan, 1995). As previously discussed (Faeder et al., 2003), to equalize the comparison, the levels of phosphorylation are plotted as a function of the number of receptors in aggregates. Figure 11a shows the ligand concentrations needed to achieve the same level of receptor aggregation for the different ligands. As k_{off} is increased while keeping $k_{+2}R_T$ fixed, for both bivalent and trivalent ligands, a higher ligand concentration is required to yield the same number of aggregated receptors, since the rate at which the receptor cross-link is broken is enhanced, whereas the rate at which the cross-links form remains unaltered. In Figure 11d we see that as the lifetime of a receptor in an aggregate is decreased, i.e., k_{off} is increased, full Syk activation is dramatically reduced for both bivalent and trivalent ligands. Kinetic proofreading dominates any positive effects serial engagement may have on Syk activation. This result is similar to that seen in experiments using fast and slowly dissociating multivalent ligands that aggregate IgE on RBL cells (Torigoe et al., 1998).

Figure 11b and Figure 11c show that the proximal signaling events, β and γ ITAM phosphorylation, compared with Syk phosphorylation, are effected less by the changes in the ligand-receptor lifetime as expected from a kinetic proofreading model (McKeithan, 1995). The reduction in Syk phosphorylation is pronounced because it is much further down the signaling cascade than phosphorylation of the receptor γ-chain. A number of reversible steps must occur to go from γ-chain phosphorylation to Syk phosphorylation. A Syk molecule has to bind to a phosphorylated γ-chain before the γ-chain is dephosphorylated. For transphosphorylation of the γ-bound Syk molecule to occur, a second Syk molecule must bind, which requires a second γ-chain to be phosphorylated in the same aggregate. Finally, transphoshorylation among the Syk molecules must occur before either of the Syk molecules dissociates.

4.3.2 Increasing serial engagement by increasing k_{+2} increases Syk activation

In Figure 12 we compare the levels of β and γ ITAM phosphorylation and full Syk activation induced by four different hypothetical ligands, two bivalent (circles) and two trivalent

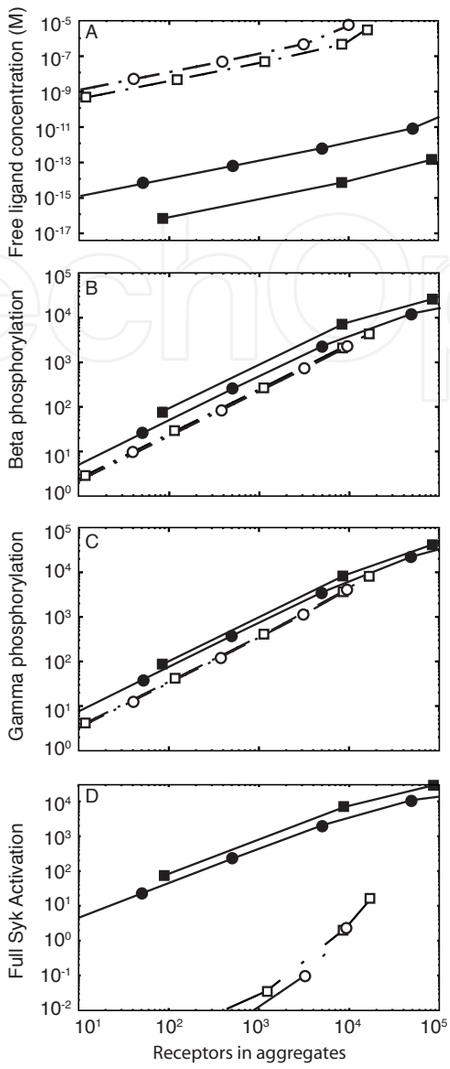

Fig. 11. Simulation of the effects of increasing the rate of serial engagement of bivalent and trivalent ligand by increasing the ligand-receptor dissociation constant, k_{off}. The four curves correspond to $k_{+2}R_T = 1.0\ \text{s}^{-1}$ and bivalent (circles) and trivalent (squares) ligands with $k_{\text{off}} = 0.01\ \text{s}^{-1}$ (solid lines and symbols) and $10\ \text{s}^{-1}$ (dashed lines and open symbols). The additional parameters used in the simulations are given in Table I of Faeder et al. (2003). The x-axis indicates levels of FcϵRI aggregation, given as the number of receptors per cell in aggregates. One percent of the cell's receptors in aggregates corresponds to 4×10^3 receptors. (A) Free ligand concentrations corresponding to specified levels of receptor aggregation. (B), (C), and (D) are respectively the predicted number of receptors per cell with the β ITAM phosphorylated, the γ ITAM phosphorylated, and Syk bound to the phosphorylated γ ITAM and transphosphorylated on its activation loop by another Syk.

(squares), that have the same dissociation rate constant $k_{\text{off}} = 0.1\ \text{s}^{-1}$ and different surface cross-linking constants. Each pair of bivalent and trivalent ligands have surface cross-linking constants such that $k_{+2}R_T = 0.1\ \text{s}^{-1}$ (solid lines and symbols) and $100\ \text{s}^{-1}$ (dashed lines and

open symbols). As in Figure 11, we compare ligands at different concentrations that result in the same number of receptors being in aggregates at equilibrium. Since k_{off} is fixed, the lifetime of a receptor in an aggregate is the same for all four ligands. As $k_{+2}R_T$ is increased from 0.1 s^{-1} to 100 s^{-1}, the rate of serial engagement for the bivalent ligand increases from 0.067 s^{-1} to 0.20 s^{-1} (Eq.(38)), and for the trivalent ligand from 0.13 s^{-1} to 0.30 s^{-1} (Eq.(39)). (These rates of serial engagement were calculated for low ligand concentrations, when $R \approx R_T$ and $k_{+2}R \approx k_{+2}R_T$.) We see that the simulations predict that increasing the rate of serial engagement while holding k_{off} fixed has a minor effect on receptor phosphorylation (12b and c), but a more pronounced effect on the phosphorylation of Syk by Syk, i.e, on full Syk activation (12d).

4.3.3 Increasing the valence of a ligand increases Syk activation, partly as a result of increased serial engagement

From Eqs. (38) and (39) we can calculate the increase in the rate of serial engagement as a result of increasing the valence of a ligand from two to three while keeping its rate constants unchanged. The factor by which the rate of serial engagement increases, r_3/r_2, depends only on the parameter $k_{+2}R$, and monotonically decreases from 2 to 3/2 as $k_{+2}R$ increases from zero to infinity. In Figure 13, as in 12, we compare the predicted full Syk activation from simulations where the stimulating ligand is either bivalent (circles) or trivalent (squares), the rate of serial engagement is varied by varying k_{+2}, and for both ligands, the lifetime of a receptor bound to a ligand is the same, 10 s ($k_{\text{off}} = 0.10\ s^{-1}$). The range over which the rate of serial engagement varies in Figure 13 corresponds to $k_{+2}R = 0.01 - 100\ s^{-1}$. In Figure 13a, the two top curves and two bottom curves correspond to 1000 and a 100 receptors per cell in aggregates. For the same rate of serial engagement and the same number of receptors in aggregates, the model predicts that the trivalent ligand is more effective than the bivalent ligand at activating Syk.

In Figure 13b, we re-plot the simulations for the upper two curves in Figure 13a. To illustrate how we can asses the contribution of serial engagement in enhancing Syk phosphorylation of Syk when the valence is increased, we consider the point labeled 1 on the Syk activation curve for the bivalent ligand in Figure 13b. This point corresponds to the serial engagement rate for a bivalent ligand with $k_{+2}R = 0.01\ s^{-1}$ and $k_{\text{off}} = 0.10\ s^{-1}$. When the valence is increased from two to three with the rate constants unchanged, the rate of serial engagement for the trimer increases above that of the dimer to the point on the trivalent ligand curve labeled 2. We see that there would be an increase in Syk phosphorylation of Syk for a trivalent ligand even if there was no increase in the rate of serial engagement. This is indicated by the difference B-A on the y-axis and is a result of effects other than serial engagement. The increase in Syk activation that is attributable to the increase in serial engagement is indicated by the difference C-B on the y-axis, which can be substantial.

Lyn is strongly regulated by Cbp and Csk (Kawabuchi et al., 2000; Ohtake et al., 2002) on RBL cells and as a result, the amount of Lyn available to the receptor is in short supply (Torigoe et al., 1997; Wofsy et al., 1997). Although Lyn regulation is not in the model, the Lyn concentration available to the receptor is chosen so that Lyn is limiting. In the model, in the absence of the ligand, less than five percent of the receptors are associated with Lyn which is consistent with the observations of Yamashita et al. (Yamashita et al., 1994). Upon aggregation, large receptor aggregates are more likely to contain a Lyn than small receptor aggregates, and once a Lyn is in an aggregate it can transphosphorylate all receptors in its proximity. It is

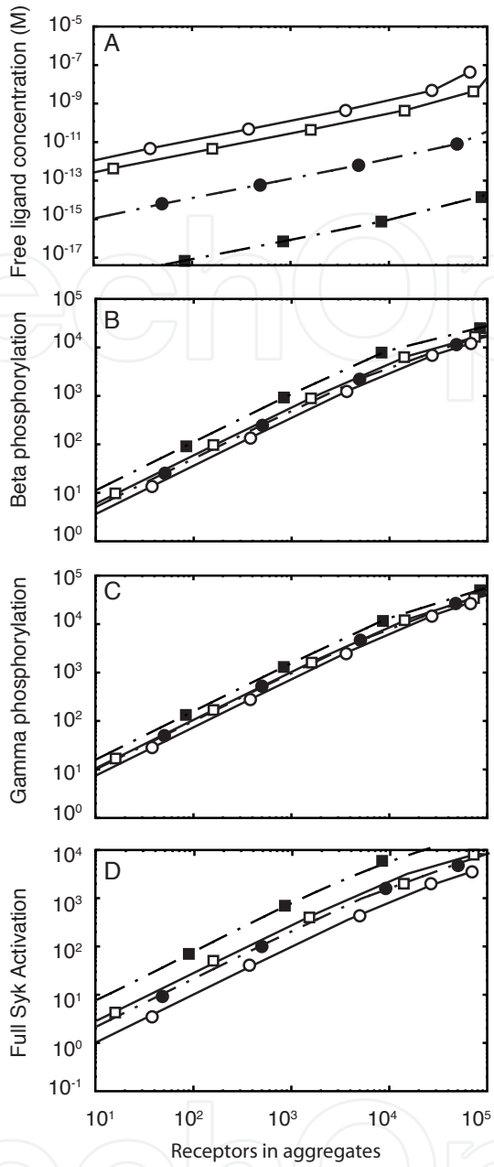

Fig. 12. Simulation of the effects of increasing the rate of serial engagement of bivalent and trivalent ligand by increasing the rate of crosslinking, $k_{+2}R$. The four curves correspond to $k_{\text{off}} = 0.1\ \text{s}^{-1}$ and bivalent (circles) and trivalent (squares) ligands with $k_{+2}R = 0.1\ \text{s}^{-1}$ (solid lines and symbols) and $100\ \text{s}^{-1}$ (dashed lines and open symbols). All other parameters are the same as in Figure 11. The x-axis indicates levels of FcϵRI aggregation, given as the number of receptors per cell in aggregates. (A) Free ligand concentrations corresponding to specified levels of receptor aggregation. (B), (C), and (D) are respecitively the predicted number of receptors per cell with the β ITAM phosphorylated, the γ ITAM phosphorylated, and Syk bound to the γ ITAM and transphosphorylated by Syk on its activation loop.

these effects that the model captures when the valence of the ligand is increased from two to three and that account for the increase in Syk phosphorylation that is not a result of serial

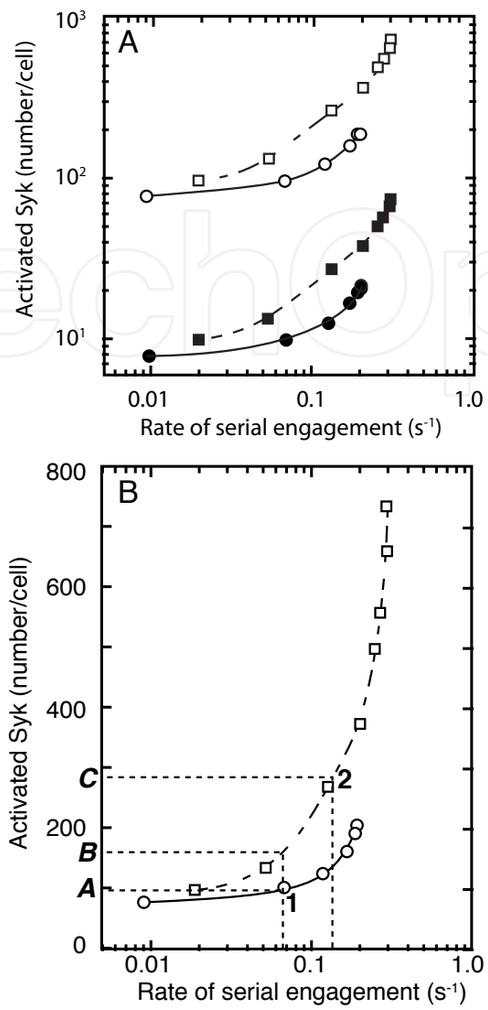

Fig. 13. Predicted number of activated Syk (Syk transphosphorylated by Syk) as a function of the rate of serial engagement. (A) The circles refer to bivalent ligand simulations and the squares to trivalent ligand simulations. Open and solid symbols refer to 1000 and 100 receptors in aggregates respectively. (B) Replot of the bivalent and trivalent curves in (A) for 1000 receptors in aggregates. The symbol 1 corresponds to a dimer with $k_{+2}R = 0.01\ \mathrm{s}^{-1}$ and $k_{\mathrm{off}} = 0.10\ \mathrm{s}^{-1}$. The symbol 2 corresponds to a trimer with the same rate constants. $A = 100$, $B = 161$ and $C = 290$ activated Syk per cell. The net increase in activated Syk, $(C - A)$ is 190 Syk per cell, of which $C - B = 129$ Syk per cell can be attributed to serial engagement.

engagement. We investigate this further by considering ligands that cannot serial engage receptors.

4.3.4 Serial engagement is not necessary for Syk activation

Although the aggregation of FcϵRI is an absolute requirement for mast cell signaling mediated by FcϵRI, serial engagement is not, as has been demonstrated using oligomers of IgE (Kent et al., 1994). As a test of our model, we have carried out simulations with bivalent and

trivalent oligomers of IgE considered as ligands, taking the dissociation rate constant $k_{off} = 0$, which ensures that there is no serial engagement. (Since the half-life for dissociation of an IgE-Fcϵ complex is close to a day (Kulczycki & Metzger, 1974), this is an excellent approximation in simulating experiments that last a few hours or less.) The predicted results for γ-phosphorylation and Syk activation for IgE dimers and trimers at one hour are shown in Figures 14a and 14b. These results are compared to histamine release dose response curves for RBL-2H3 cells exposed to IgE oligomers for one hour. Because of the slow forward rate constant for IgE binding to FcϵRI (Wofsy et al., 1995), equilibrium is achieved at one hour only for IgE concentrations greater than about 5 μg/ml. The simulations indicate that to achieve measureable histamine release from RBL cells requires the activation of substantial numbers of Syk molecules. For example, the simulations predict that 10% histamine release with trivalent ligands, about 25% of maximal release, occurs when approximately 10,000 Syk are fully activated.

5. Discussion

Mutivalent ligands (allergens) bind to, and aggregate, IgE complexed with FcϵRI receptors expressed on the surface of mast cells and basophils. We have used a generalized version of the model of Faeder et al. (2003) of the early cell signaling events (seconds to minutes) mediated by the cross-linking of IgE-FcϵRI complexes to study the dependence of the activation of Syk on the cellular concentrations of Syk and IgE-FcϵRI complexes and to investigate the role of serial engagement in Syk activation. The model was originally developed for covalently cross-linked dimers of IgE binding to FcϵRI on the surface of RBL cells (Faeder et al., 2003). For bivalent ligands binding reversibly to IgE-FcϵRI complexes, the model applies when IgE acts as a monovalent receptor. We restrict the use of the model to concentrations of bivalent ligands for which the binding of two ligands to one IgE is negligible. In the model, full activation of Syk can only occur when two Syk molecules are bound to a receptor dimer formed by a bivalent ligand. A Syk molecule becomes fully activated when it is *transphosphorylated* on its activation loop tyrosines (Tyr^{518} and Tyr^{519} in murine Syk) by a Syk bound to the adjacent receptor in the dimer. Using antibodies specific for phosphorylated tyrosines in the activation loop of Syk, Zhang et al. (Zhang et al., 2000) showed that upon FcϵRI aggregation, these tyrosines became phosphorylated and the extent of phosphorylation depended on the kinase activity of Syk. Further, the presence of these activation loop tyrosines was necessary for Syk-mediated propagation of FcϵRI signaling (Zhang et al., 1998). Syk is capable of phosphorylating its activation loop tyrosines both *in vitro* (Tsang et al., 2008; Zhang et al., 2000) and *in vivo* Zhang et al. (2000), but it is still unresolved whether transphosphorylation (phosphorylation of one Syk molecule by another in the same complex) or autophosphorylation (phosphorylation of a Syk molecule by the kinase domain of the same molecule) is the mechanism by which the Syk activation loop tyrosines are phosphorylated in mast cells and basophils.

If the mechanism of Syk activation is Syk transphosphorylation of Syk, as postulated by Faeder et al. (2003), the Syk activation curve can be either bell-shaped or double-humped, depending on the cellular concentrations of Syk and IgE-FcϵRI complexes (see Figure 2). On the other hand, if Syk activation is achieved via autophosphorylation, the model predicts that only a bell-shaped Syk activation curve is possible. In the model, it is assumed that because of steric hindrance only one Syk molecule can bind per receptor, even though there are two disulfide-linked γ-chains that, when fully phosphorylated, present two binding sites for Syk.

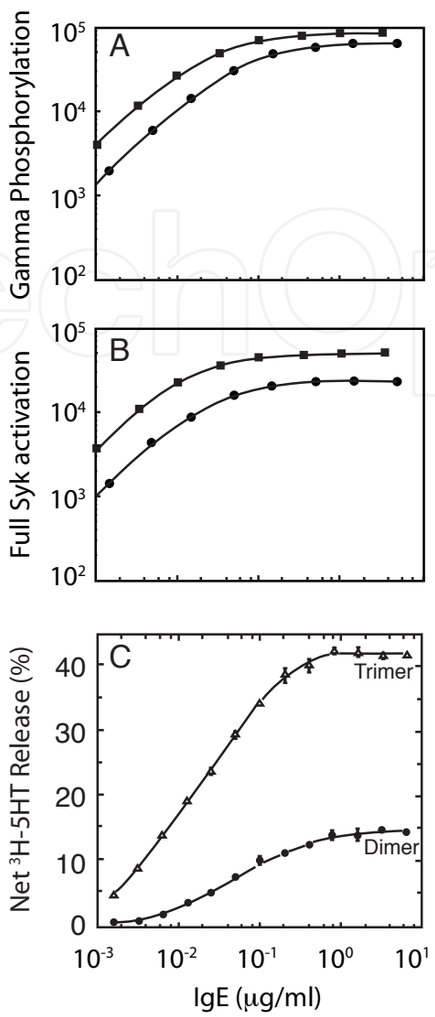

Fig. 14. Predicted γ and Syk phosphorylation, and measured RBL-2H3 cell degranulation, for dimeric and trimer oligomers of IgE. In (A) and (B) the circles refer to IgE dimer simulations and the squares to IgE trimer simulations. The rate constants characterizing the oligomers are taken to be $k_{\text{off}} = 0\ \text{s}^{-1}$, $k_{+1} = 8 \times 10^4\ \text{M}^{-1}\ \text{s}^{-1}$ and $k_{+2}R_T = 100\ \text{s}^{-1}$. The simulations correspond to exposure of the ligands to RBL-2H3 cells for one hour. (C) Experimentally determined degranulation of RBL-2H3 cells after one hour of exposure to either dimers or trimers of IgE (Fewtrell & Metzger, 1980).

If two Syk can be bound simultaneously to the same receptor on two separate γ-chains, and if they can transphosphorylate each other to achieve full Syk activation, the prediction is still that Syk activation curves can be either bell-shaped or double humped depending on the ratio of the receptor to Syk concentrations.

Unfortunately, at present there are no experimentally-determined Syk activation curves to help us distinguish among possible mechanisms for the phosphorylation of the Syk activation loop tyrosines. If we look further downstream than Syk activation at histamine release from basophils, which requires kinase active Syk, the data are consistent with the Syk

transphosphorylation mechanism. For example, although most histamine release curves show only a single maximum, double-humped histamine release curves have been observed (Delisi & Siraganian, 1979; Weyer et al., 1982). (Histamine release curves are plots of the fraction of a cell's total histamine that is released in a given time versus the logarithm of the concentration of ligand the cell is exposed to.) In addition, for ligand concentrations where receptor aggregate formation is high and histamine release low, the addition of monovalent hapten, which reduces the number of receptors in dimers, increases histamine release (Magro & Alexander, 1974; Magro & Bennich, 1977). In model simulations, the same manipulation increases Syk activation (Figure 4).

To study the properties of Syk activation, we performed simulations over a range of ligand concentrations for different Syk and receptor concentrations. From the simulations we found that even though the receptor cross-linking curve was symmetric with respect to the log of the ligand concentration in the steady state (Figure 15), the Syk activation curve often was not. This was easiest to see when the Syk activation curve was doubled-humped (Figure 5). The asymmetry in the steady state occured when, at two different ligand concentrations yielding identical total numbers of receptors in dimers and identical lifetimes of a receptor in a dimer, the levels of Syk activation differed. This was puzzling since all that differed on the cell surface at the two ligand concentrations was the number of receptors bound monovalently. Why should this matter since basophils and mast cells don't respond to monovalently bound ligand? The answer is subtle and concerns the competition between kinetic proofreading, that activation requires the receptor to undergo multiple binding and chemical modification events while the receptor is in an aggregate, and serial engagement, that ligands can bind multiple receptors before dissociating from the cell surface.

Once a receptor dimer breaks up, the two receptors, one with a ligand attached and the other free, will diffuse away from each other. If Syk or Lyn is bound to the receptors, these kinases will dissociate with half-lives of about ten seconds, leaving behind unprotected ITAM phosphotyrosines to be rapidly dephosphorylated. Thus, the receptors would return to their basal state. If, however, a receptor can re-form a dimer before it has been transformed back to its basal state, it can partially compensate for the effects of kinetic proofreading. The asymmetry in the Syk activation curve arises because the minimum time required by a receptor to form a dimer is dependent on the free ligand concentration (Figure 9). At low ligand concentration, and therefore low numbers of bound receptors, a singly bound receptor will collide with many free receptors and have ample opportunity to rapidly form a dimer. At high ligand concentration, and therefore low numbers of free receptors, a free receptor will have many bound receptors to collide with, but, because the free ligand concentration is high, the free receptor may bind a ligand from solution before it has time to form a dimer. Thus, at low ligand concentration, re-formation of dimers is more effective than at high ligand concentration at reducing the effects of kinetic proofreading. In our simulations, the double-humped Syk activation curves (Figure 5) show that Syk activation can be higher at the first maximum (at the lower ligand concentration) than at the second maximum (at the higher ligand concentration) where the extent of receptor cross-linking is the same at both maxima.

To further probe the underlying mechanism of the asymmetry in the Syk activation curve, we considered our model in the limit when Lyn is in large excess and γ-ITAM phosphorylation follows immediately upon dimer formation. In this limit, simulations again showed an asymmetry in the double-humped Syk activation curve (Fig.6a). Since for full Syk activation to occur, a Syk dimer (Syk-FcϵRI-ligand-FcϵRI-Syk) must form, we calculate the mean time

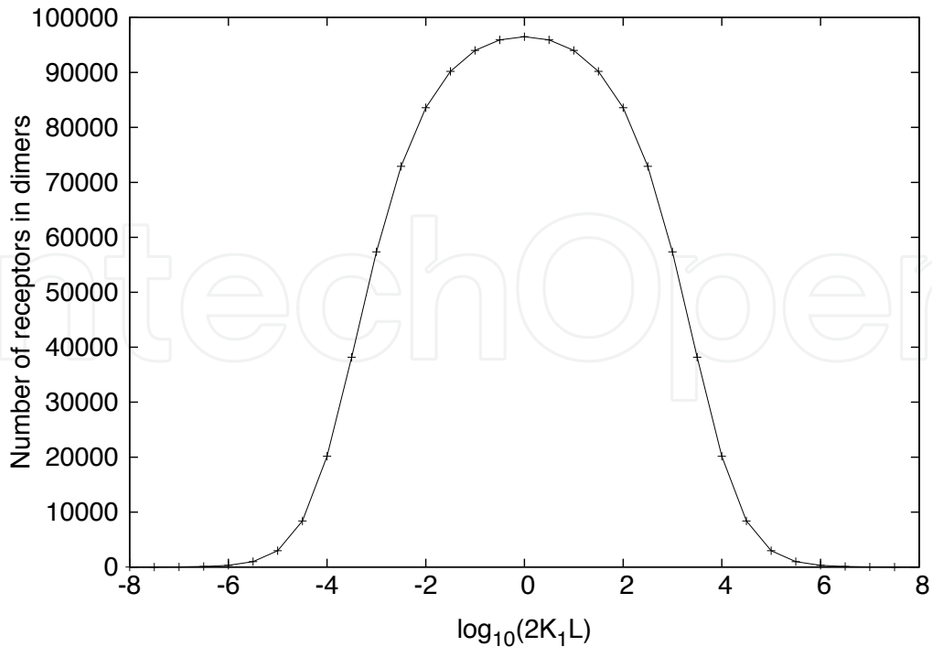

Fig. 15. Receptor cross-linking (dimerization) curve for $k_{+1} = 2.5 \times 10^7$ M^{-1} s^{-1}; $k_{+2} = 8 \times 10^{-9} cm^2 s^{-1}$; $k_{-1} = 0.316(10^{-0.5})$ s^{-1}, $k_{-2} = 0.0316(10^{-1.5})$ s^{-1}. The receptor aggregation is maximum at $L = 1/2K_1$, i.e. at $\log_{10}(2K_1L) = 0$, where $K_1 = k_{+1}/k_{-1}$ is the equilibrium constant for the extracellular bivalent ligand, present at concentration L, for binding to the Fab part of the IgE.

for a Syk molecule that is not in a Syk dimer to be incorporated into a Syk dimer. The time for this to occur showed a similar asymmetry as that of the minimum time for a receptor to enter a dimer. It appears that the asymmetry in the Syk activation curve is a manifestation of the underlying competition that is constantly occurring between kinetic proofreading and serial engagement in signaling cascades triggered by multivalent ligands aggregating cell surface receptors.

The asymmetry we observed in simulations of Syk activation curves was always small. Although the explanation of the effect is interesting, whether it is ever important in cell signaling is an open question. Since amplifications of cell signals can be highly nonlinear, it is possible that small differences in the concentration of activated kinases early in a signaling cascade can have profound effects on later cell responses.

A major function of activated Syk in mast cells and basophils is to phosphorylate a set of tyrosines on the transmembrane adapter protein LAT (linker for the activation of T cells). LAT's three distal tyrosines, when phosphorylated, all bind the adapter protein Grb2, and Grb2 mediates the aggregation of LAT (Houtman et al., 2006). The size of the LAT aggregates that form depends strongly on whether or not all three of the Grb2 binding site tyrosines are phosphorylated (Nag et al., 2009). It remains to be seen whether small differences in the amount of activated Syk can lead to large differences in the distribution of LAT aggregates that form downstream of Syk.

The model prediction of differential Syk activation at low and high extracellular ligand concentrations, which arises from differential compensation by serial engagement for the effects of kinetics proofreading at the two ligand concentrations, has led us to explore in greater detail, the role of serial engagement in enhancing Syk activation in mast cells and basophils. When surface densities of receptors are sufficiently high, multivalent ligands can bind to cell surfaces and serial engage numerous receptors before dissociating, i.e., before all of the ligand's binding sites are simultaneously free. Even with a valence as low as two, a ligand can engage multiple receptors from the time it first attaches to the surface until the time it dissociates (see Table 3). A single binding site on a ligand may bind a receptor, dissociate from it, and repeat the cycle with a new receptor multiple times before the ligand leaves the surface.

Using our detailed mathematical model, we have investigated the role of serial engagement of FcϵRI in mast cell signaling. We use the model for low concentrations of the multivalent ligand so that the binding of two ligands to one IgE is negligible. For the purpose of exploring the role of serial engagement in enhancing Syk activation, we have included in our model, cross-linking reactions between a trivalent ligand and an IgE-FcϵRI complex. The concentration of receptors is chosen to be high enough that there is a significant population of free receptors so that serial engagement is favored. A basic assumption of the model is that when a ligand is bound to more than one receptor and a bond opens, the freed receptor diffuses away before the site on the ligand can rebind to it. This is a reasonable assumption as long as receptors remain mobile on the cell surface. Receptors in small aggregates on the RBL cell surface remain mobile (Andrews et al., 2009), but not the receptors in large aggregates (Andrews et al., 2008; Menon et al., 1986). We expect serial engagement to be significantly reduced and exert little effect on cell signaling when the surface receptors are immobile. We have only considered the case when receptors remain mobile and our results do not apply to large aggregates where receptors are immobile. The expression we have derived for the rate of serial engagement for a ligand of valence N, Eq. (37), holds only when receptors are mobile.

We considered three ways in which serial engagement could be enhanced: by increasing the rate at which a ligand binding site dissociates from a receptor; by increasing the rate at which a free site on a ligand that is bound to a receptor can cross-link another receptor; and by increasing the valence of the ligand. Model simulations showed that increasing the rate of serial engagement by increasing the rate of dissociation reduced the concentration of activated Syk (see Figure 11d). Increasing the rate of dissociation of a ligand-receptor bond decreases the lifetime of a receptor in an aggregate and accentuates the effect of kinetic proofreading. The further down the signaling pathway an event occurs, the more pronounced are the effects of kinetic proofreading on the event, as can be seen by comparing the predicted γ-chain phosphorylation (Figure 11c) with the predicted Syk phosphorylation (Figure 11d). The positive effects serial engagement has on signaling are outweighed by kinetic proofreading when the lifetime of the ligand-receptor bond is decreased(McKeithan, 1995; Torigoe et al., 1998).

Simulations predict that increasing the rate at which cross-linking occurs, while keeping the lifetime of the bond between a ligand site and receptor constant, so as not to enhance kinetic proofreading, increases Syk activation. In Figure 13a, a single curve corresponds to a series of bivalent or trivalent ligands with increasing rates of serial engagement achieved by increasing cross-linking constants. The ligands have the same dissociation rate constants and

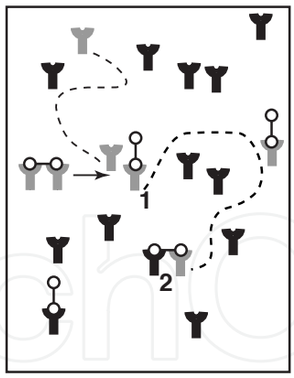

Fig. 16. At low ligand concentration, when most receptors are unbound, a receptor-ligand complex that dissociates from an aggregate (1), can rapidly enter a new aggregate (2), provided that the rate of cross-linking is greater than the rate of dissociation of its ligand-receptor bond. If this is not the case the ligand-receptor complex will be rapidly converted to a free receptor, reducing it chance of quickly finding a binding partner.

their concentrations have been chosen so that they aggregate the same number of receptors on the cell surface, yet the faster the ligands are able to serial engage receptors, the more Syk they are able to activate. This model prediction supports the hypothesis used to explain the previously discussed asymmetric Syk activation profile, that serial engagement can partially nullify the effects of kinetic proofreading by allowing receptors that have dissociated from an aggregate to enter new aggregates before they fully return to their basal state. Previously we estimated that when a receptor leaves an aggregate its unprotected phosphotyrosines are dephosphorylated in less than a second, and any Syk or Lyn that are bound to phosphorylated ITAMS dissociate with half-lives of the order of 10-15 seconds (Faeder et al., 2003). Even within an aggregate, phosphorylation and dephosphorylation is constantly occurring (Kent et al., 1994). If a receptor can enter into a new aggregate before all the modifications it has undergone have been reversed, full activation of Syk will be more efficient.

As depicted in Figure 16 for a bivalent ligand at low concentration, a receptor that remains bound to a ligand when an aggregate breaks up is much more likely to be rapidly incorporated into a new aggregate than a receptor with its binding site free, provided the rate for cross-linking a new receptor is equal to, or faster than the rate of dissociation of the ligand-receptor bond, i.e., $k_{+2}R \geq k_{\text{off}}$, or equivalently $K_2R \geq 1$. Even when this condition on the rate constants is met, serial engagement can only partially compensate for the effects of kinetic proofreading since free receptors that leave an aggregate will most likely return to the basal state before they form new aggregates.

The model also predicts that increasing the valence of a ligand from two to three, while keeping the rate constants the same, increases Syk activation (Figure 13). We have derived expressions for the rates of serial engagement of dimers and trimers, Eqs. (38) and (39), which show that increasing the valence while keeping all other quantities fixed raises the rate of serial engagement. However, the predicted increase in Syk activation is not solely due to the increase in serial engagement. Both experiment (Fewtrell & Metzger, 1980) and the model predictions (Figure 14) indicate that trimeric oligomers of IgE are more effective than dimers at activating RBL cells, even though these ligands cannot serial engage receptors. This is because

Lyn is limiting in RBL cells, with most receptors not associated with a Lyn (Torigoe et al., 1997; Wofsy et al., 1997; Yamashita et al., 1994). Large aggregates are more likely than small aggregates to have a Lyn bound to a receptor in the aggregate and initiate signaling. Further, the larger the aggregate, the higher is the number of receptors that can be phosphorylated by a single Lyn. Serial engagement can further accentuate this signaling. We have estimated the additional contribution to Syk activation from the increase in serial engagement when a trivalent ligand is substituted for a bivalent ligand and shown that it can be substantial (Figure 13b).

Ligand-induced receptor aggregation initiates a chemical cascade that involves chemical reactions that build and use transient molecular scaffolds. Upon aggregation of FcϵRI on mast cells, the cytoplasmic domains of the receptor become sites for the coalescence of the kinases Lyn and Syk, with Syk undergoing rapid activation by phosphorylation. The activated Syk phosphorylates conserved tyrosines on adaptor molecules such as LAT to form scaffolding molecules. However, the structures formed around the cytoplasmic domains of the receptor, as well as other scaffolding proteins, are ephemeral with components going on and off rapidly. How successful this construction will be depends on the lifetime of a receptor in an aggregate. If the lifetime is too short, most of the chemical cascades that are initiated will not go to completion, and signaling will be dampened or completely prevented. This is the idea behind kinetic proofreading (reviewed in (Goldstein et al., 2008)), introduced in the context of cell signaling by McKeithan (McKeithan, 1995), and kinetic proofreading has highlighted the role of the pMHC-TCR bond dissociation rate constant in T-cell signaling. We have used a mathematical model of the initial steps in the chemical cascade triggered by FcϵRI aggregation on mast cells to investigate the role of serial engagement in signaling, and shown that for a series of ligands with the same dissociation rate constant, increasing the forward rate constant for cross-linking, or increasing the ligand valence increases serial engagement and Syk activation. Serial engagement is able to partially reverse the effects of kinetic proofreading and enhance mast cell signaling.

6. Conclusion

Faeder et al. have developed detailed mathematical model of the early signaling events, up to and including Syk activation, that are triggered when IgE-FcϵRI complexes are exposed to a bivalent or trivalent ligand on rat basophilic leukemia (RBL) cells. We have used this model to investigate the effect of cellular Syk and FcϵRI concentrations on the level of Syk activation. Using model simulations, we show that for a subset of physiological FcϵRI and Syk concentrations, differences in total extracellular ligand concentration can lead to subtle kinetic effects that yield qualitative differences in the levels of Syk activation. Since these kinetic effects arise from differential serial engagement rates at different ligand concentrations, we have assessed the contribution of serial engagement to Syk activation in mast cells and basophils, and shown that for a series of ligands with the same dissociation rate constant, increasing the forward rate constant for cross-linking, or increasing the ligand valence increases serial engagement and Syk activation. Serial engagement is able to partially reverse the effects of kinetic proofreading and enhance mast cell signaling. To summarize, we review in this chapter, our research directed at determining the possible factors that influence the levels of Syk activation in mast cells and basophils. Syk activation is a crucial step in the signal transduction cascade in mast cells and basophils that gives rise to the allergic response in individuals. An in-depth understanding of the strength of the signal transduced

via this biochemical network, and its underlying kinetics, will be of immense assistance in a network level approach for design of allergy drugs that targets multiple molecules in the signal transduction cascade.

7. Acknowledgements

This work was supported by NIH Grant R37-GM035556 and by the Department of Energy through contract W-7405-ENG-36. MLB received partial supported from NIH Grants R01 GM076570 and NIH U54 RR022232 . The authors have no financial conflict of interest.

8. References

Aleksic, M., Dushek, O., Zhang, H., Shenderov, E., Chen, J.-L.and Cerundolo, V., Coombs, D. & van der Merwe, P. A. (2010). Dependence of T cell antigen recognition on TCR/pMHC confinement time, *Immunity* 32: 163–174.

Andrews, N. L., Lidke, K. A., Pfeiffer, J. R., Burns, A. R., Wilson, B. S., Oliver, J. M. & Lidke, D. S. (2008). Actin restricts FcϵRI diffusion and facilitates antigen-induced receptor immobilization, *Nature Cell Biol.* 10: 955–962.

Andrews, N. L., Pfeiffer, J. R., Martinez, A. M., Haaland, D. M., Davis, R. W., Kawakami, T., Oliver, J. M., Wilson, B. S. & Lidke, D. S. (2009). Small, mobile FcϵRI aggregates are signaling competent., *Immunity* 31: 469–479.

Becker, K., Ishizaka, T., Metzger, H., Ishizaka, K. & Grimley, P. (1973). Surface IgE on human basophils during histamine release, *J. Exp. Med.* 138: 394–409.

Benhamou, M., Ryba, N. J. P., Kihara, H., Nishikata, H. & Siraganian, R. P. (1993). Protein-tyrosine kinase $p72^{Syk}$ in high-affinity IgE receptor signaling: identification of a component of pp72 and association with the receptor γ chain after receptor agregation, *J. Biol. Chem.* 268: 23318–23324.

Blank, U., Ra, C., Miller, L., White, K., Metzger, H. & Kinet, J. (1989). Complete structure and expression in transfected cells of high affinity IgE receptor, *Nature* 337: 187–189.

Blinov, M. L., Faeder, J. R., Goldstein, B. & Hlavacek, W. S. (2004). Bionetgen: Software for rule-based modeling of signal transduction based on the interactions of molecular domains, *Bioinformatics* 20: 3289–3292.

Carreno, L. J., Bueno, S. M., P., B., Nathenson, S. G. & Kalergis, A. M. (2007). The half-life of the T-cell receptor/peptide-major histocompatibility complex interaction can modulate T-cell activation in response to bacterial challenge., *Immunol.* 121: 227–237.

Coombs, D. & Goldstein, B. (2005). T cell activation: Kinetic proofreading, serial engagement and cell adhesion., *J. Comput. Appl. Math.* 184: 121–139.

Coombs, D., Kalergis, A. M., Nathenson, S. G., Wofsy, C. & Goldstein, B. (2002). Activated TCR remain marked for internalization after dissociation from peptide-MHC, *Nat. Immunol.* 3: 926–931.

Davis, M. M. (1995). Serial engagement proposed, *Nature* 375: 104.

de Castro, R. (2011). Regulation and function of syk tyrosine kinase in mast cell signaling and beyond, *J. Signal Transduct.* 2011(507291): 1–9.

de Castro, R., Zhang, J., Jamur, M., Oliver, C. & Siraganian, R. (2010). Tyrosines in the Carboxyl Terminus Regulate Syk Kinase Activity and Function, *J. Biol. Chem.* 285: 26674–26684.

Delisi, C. & Siraganian, R. (1979). Receptor cross-linking and histamine release. ii. interpretation and analysis of anomalous dose response patterns, *J. Immunol.* 122: 2293–2299.

Dembo, M. & Golstein, B. (1978). Theory of Equilibrium Binding of Symmetric Bivalent Haptens to Cell Surface Antibody: Application to Histamine Release from Basophils, *J. Immunol.* 121: 345–353.

Faeder, J. R., Blinov, M. L. & Hlavacek, W. S. (2009). Rule-based modeling of biochemical systems with BioNetGen., *Methods Mol. Biol.* 500: 113–167.

Faeder, J. R., Hlavacek, W. S., Reischl, I., Blinov, M. L., Metzger, H., Redondo, A., Wofsy, C. & Goldstein, B. (2003). Investigation of early events in FcεRI-mediated signaling using a detailed mathematical model., *J. Immunol.* 170: 3769–3781.

Fewtrell, C. & Metzger, H. (1980). Larger oligomers of IgE are more effective than dimers in stimulating rat basophilic leukemia cells, *J. Immunol.* 125: 701–710.

Goldstein, B., Coombs, D., Faeder, J. R. & Hlavacek, W. S. (2008). Kinetic proofreading model, *Adv. Exp. Med. Biol.* 640: 82–94.

Goldstein, B. & Wofsy, C. (1994). Aggregation of cell surface receptors, *Lectures on Mathematics in the Life Sciences* 24: 109–135.

Gopalakrishnan, P. V. & Karush, F. (1974). Antibody affinity VII. Multivalent interaction of anti-lactoside antibody, *J. Immunol.* 113: 769–778.

Greenbury, C. L., Moore, D. H. & Nunn, A. C. (1965). The reaction with red cells of 7S antibody. Its subunits and their recombinants., *Immunology* 8: 420–431.

Hlavacek, W., Faeder, J., Blinov, M., Perelson, A. & Goldstein, B. (2003). The Complexity of Complexes in Signal Transduction, *Biotechnolgy and Bioengineering* 84: 783–794.

Hlavacek, W. S., Percus, J. K., Percus, O. E., Perelson, A. S. & Wofsy, C. (2002). Retention of antigen on follicular dendritic cells and B lymphocytes through complement-mediated multivalent ligand-receptor interactions: theory and application to HIV treatment, *Math. Biosci.* 176: 185–202.

Hlavacek, W. S., Wofsy, C. & Perelson, A. S. (1999). Dissociation of HIV-1 from follicular dendritic cells during HAART: Mathematical analysis, *Proc. Natl. Acad. Sci. USA* 96: 14681–14686.

Hong, J. J., Yankee, T. M., Harrison, M. L. & Geahlen, R. L. (2002). Regulation of signaling in B cells through the phosphorylation of Syk on linker-region tyrosines. A mechanism for negative signaling by the Lyn tyrosine kinase, *J. Biol. Chem.* 277: 31703–31714.

Hornick, C. L. & Karusch, F. (1972). Antibody affinity III. The role of multivalence., *Immunochem.* 9: 325–340.

Houtman, J. C., Yamaguchi, H., Barda-Saad, M., Braiman, A., Bowden, B., Appella, E., Schuck, P. & Samelson, L. E. (2006). Oligomerization of signaling complexes by the multipoint binding of GRB2 to both LAT and SOS1, *Nat. Struct. Mol. Biol.* 13: 798–805.

Hutchcroft, J. E., Geahlen, R. H., G., D. G. & Oliver, J. M. (1992). Fcεri-mediated tyrosine phosphorylation and activation of the 72-kDa protein-tyrosine kinase, PTK72, in RBL-2H3 rat-tumor mast cells, *Proc. Natl. Acad. Sci. USA* 89: 9107–9111.

Kalergis, A. M., Boucheron, N., Doucey, M. A., Palmieri, E., Goyarts, E. C., Vegh, Z., Luescher, I. F. & Nathenson, S. G. (2001). Efficient cell activation requires an optimal dwell-time of interaction between the TCR and the pMHC complex, *Nat. Immunol.* 2: 229–234.

Karush, F. (1989). The affinity of antibody: Range, variability, and the role of multivalence, *in* G. W. Litman & R. A. Good (eds), *Comprehensive Immunology 5: Immunoglobulins*, Plenum Press, New York, NY, pp. 85–116.

Kawabuchi, M., Satomi, Y., Takao, T., Shimonishi, Y., Nada, S., Nagai, K., Tarakhovsky, A. & Okada, M. (2000). Transmembrane phosphoprotein cbp regulates the activities of Src-family tyrosine kinases, *Nature* 404: 999–1003.

Kent, U. M., Mao, S.-Y., Wofsy, C., Goldstein, B., Ross, S. & Metzger, H. (1994). Dynamics of signal transduction after aggregation of cell-surface receptors: Studies on the type I receptor for igE, *Proc. Natl. Acad. Sci. USA* 91: 3087–3091.

Kulczycki, A. J. & Metzger, H. (1974). The interaction of IgE with rat basophilic leukemia cells. II. quantitative aspects of the binding reaction., *J. Exp. Med.* 140: 1676–1695.

Lanzavecchia, A., Lezzi, G. & Viola, A. (1999). From TCR engagement to T cell activation: A kinetic view of T cell behavior, *Cell* 96: 1–4.

MacGlashan Jr, D. (2007). Relationship between spleen tyrosine kinase and phosphatidylinositol 5′ phosphatase expression and secretion from human basophils in the general population, *J. Allergy Clin. Immunology* 119: 626–633.

MacGlashan Jr, D. & Lavens-Phillips, S. (2001). Characteristics of the free cytosolic calcium timelag following igE-mediated stimulation of human basophils: significance for the non-releasing basophil phenotype, *J. Leukoc. Biol.* 69: 224–232.

Magro, A. & Alexander, A. (1974). Histamine Release: In vitro studies of the inhibitory region of the dose-response curve, *J. Immunol.* 112: 1762–1765.

Magro, A. & Bennich, H. (1977). Concanavalin A induced histamine release from human basophils in vitro, *Immunology* 33: 51–58.

Mao, S.-Y. & Metzger, H. (1997). Characterization of protein-tyrosine phosphatases that dephosphorylate the high affinity receptor for IgE, *J. Biol. Chem* 272: 14067–14073.

McKeithan, K. (1995). Kinetic proofreading in T-cell receptor signal transduction., *Proc. Natl. Acad. Sci. USA* 92: 5042–5046.

Menon, A. K., Holowka, D., Webb, W. W. & Baird, B. (1986). Cross-linking of receptor-bound IgE to aggregates larger than dimers leads to rapid immobilization, *J. Cell Biol.* 102: 541–550.

Nag, A., Faeder, J. & Goldstein, B. (2010). Shaping the response: the role of fcepsilonri and syk expression levels in mast cell signalling, *IET Syst. Biol.* 4: 334–347.

Nag, A., Monine, M., Blinov, M. & Goldstein, B. (2010). A detailed mathematical model predicts that serial engagement of ige-fc epsilon ri complexes can enhance syk activation in mast cells, *J. Immunol.* 185: 3268–3276.

Nag, A., Monine, M., Faeder, J. R. & Goldstein, B. (2009). Aggergation of membrane proteins by cytosloic cross-linkers:theory and simulation of the Lat-grb2-Sos1 system, *Biophys. J.* 96: 2604–2623.

Ohtake, H., Ichikawa, N., Okada, M. & Yamashita, T. (2002). Cutting Edge:transmembrane Phosphoprotein Csk-Binding Protein/Phosphoprotein Associated With Glycosphingolipid-Enriched Microdomains as a Negative Feedback Regulator of Mast Cell Signaling Through the FcϵRI, *J. Immunol.* 168: 2087–2090.

Peirce, M. & Metzger, H. (2000). Detergent resistant microdomains offer no refuge for proteins phosphorylated by the IgE receptor, *J. Biol. Chem* 275: 34976–34982.

Rivera, J. (2005). NTAL/LAB and LAT: a balancing act in mast-cell activation and function, *Trends Immunol.* 117: 1214–1225.

Rivera, J. & Gilfillan, A. M. (2006). Molecular regulation of mast cell activation, *J. Allergy Clin. Immunol.* 117: 1214–1225.

Shiue, L., Zoller, M. J. & Brugge, J. S. (1995). Syk is activated by phosphotyrosine-containing peptides representing the tyrosine-based activation motifs of the high affinity receptor for IgE, *J. Biol. Chem.* 270: 10498–10502.

Siraganian, R., de Castro, R., Barbu, E. & Zhang, J. (2010). Mast cell signaling: The role of protein tyrosine kinase Syk, its activation and screening methods for new pathway participants, *FEBS Letters* 584: 4933–4940.

Siraganian, R., Zhang, J., Suzuki, K. & Sada, K. (2002). Protein tyrosine kinase Syk in mast cell signaling, *Mol. Immunol.* 38: 1229–1233.

Stone, J. D., Chervin, A. S. & Kranz, D. M. (2009). T-cell receptor binding affinities and kinetics: impact on T-cell activity and specificity, *Immunol.* 126: 165–176.

Taniguchi, T., Kobayashi, T., Kondo, J., Takahashi, K. et al. (1991). Molecular Cloning of a Porcine Gene *syk* That Encodes a 72-kDa Protein-Tyrosine Kinase Showing High Susceptibility to Proteolysis, *J. Biol. Chem.* 266: 15790–15796.

Torigoe, C., Goldstein, B., Wofsy, C. & Metzger, H. (1997). Shuttling of initiating kinase between discrete aggregates of the high affinity receptor for IgE regulates the cellular response, *Proc. Natl. Acad. Sci. USA* 94: 1372–1377.

Torigoe, C., Inman, J. K. & Metzger, H. (1998). An unusual mechanism for ligand antagonism, *Science* 281: 568–572.

Tsang, E., Giannetti, A., Shaw, D., Dinh, M., Tse, J., Gandhi, S. et al. (2008). Molecular mechanism of the syk activation switch, *J. Biol. Chem.* 283: 32650–32659.

Valitutti, S., Müller, S., Cella, M., Padovan, E. & Lanzavecchia, A. (1995). Serial triggering on many T-cell receptors by a few peptide-MHC complexes, *Nature* 375: 148–151.

Vonakis, B. M., Chen, H., Haleem-Smith, H. & Metzger, H. (1997). The Unique Domain as the Site on Lyn Kinase for Its Constitutive Association with the High Affinity Receptor for IgE, *J. Biol. Chem.* 272: 24072–24080.

Vonakis, B. M., Haleem-Smith, H., Benjamin, P. & Metzger, H. (2001). Interaction between the unphosphorylated receptor with high affinity for IgE and Lyn kinase, *J. Biol. Chem.* 276: 1041–1050.

Weyer, A., Dandeu, J., Marhand, F. & David, B. (1982). In vitro histamine release from human basohils triggered by a purified allergen from Dermatophagoides Farinac: Bimodel aspect of the dose response curve, *Ann. Immunol. (Paris)* 133D(1): 87–94.

Wofsy, C., Coombs, D. & Goldstein, B. (2001). Calculations show substantial serial engagement of T cell receptors, *Biophys. J.* 80: 606–612.

Wofsy, C., Kent, U. M., Mao, S.-Y., Metzger, H. & Goldstein, B. (1995). Kinetics of tyrosine phosphorylation when IgE dimers bind to Fcϵ receptors on rat basophilic leukemia cells, *J. Biol. Chem.* 270: 20264–20272.

Wofsy, C., Torigoe, C., Kent, U. M., Metzger, H. & Goldstein, B. (1997). Exploiting the Difference Between Intrinsic and Extrinsic Kinases: Implications for Regulation of Signaling by Immunoreceptors, *J. Immunol.* 159: 5984–5992.

Yamashita, T., Mao, S. & Metzger, H. (1994). Aggregation of the high-affinity IgE receptor and activation of p53/p56^{lyn} protein-tyrosine kinase, *Proc. Natl. Acad. Sci.* 91: 11251–11255.

Yang, C., Yanagi, S., Wang, X., Sakai, K., Taniguchi, T. & Yamamura, H. (1994). Purification and characterization of a protein-tyrosine kinase p72syk from porcine spleen, *Eur. J. Biochem.* 221: 973–978.

Zhang, J., Billingsley, M. L., Kincaid, R. L. & Siraganian, R. P. (2000). Phosphorylation of Syk activation loop tyrosine is essential for Syk function, *J. Biol. Chem.* 275: 35442–35447.

Zhang, J., Kimura, T. & Siraganian, R. (1998). Mutations in the activation loop tyrosines of protein tyrosine kinase Syk abrogate intracellular signaling but not kinase activity, *J. Immunol.* 161: 4366–4374.

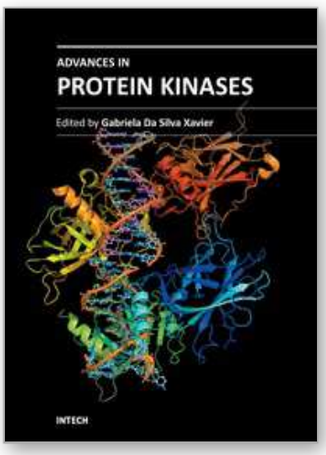

Advances in Protein Kinases

Edited by Dr. Gabriela Da Silva Xavier

ISBN 978-953-51-0633-3
Hard cover, 374 pages
Publisher InTech
Published online 05, June, 2012
Published in print edition June, 2012

Proteins are the work horses of the cell. As regulators of protein function, protein kinases are involved in the control of cellular functions via intricate signalling pathways, allowing for fine tuning of physiological functions. This book is a collaborative effort, with contribution from experts in their respective fields, reflecting the spirit of collaboration - across disciplines and borders - that exists in modern science. Here, we review the existing literature and, on occasions, provide novel data on the function of protein kinases in various systems. We also discuss the implications of these findings in the context of disease, treatment, and drug development.

How to reference

In order to correctly reference this scholarly work, feel free to copy and paste the following:

Ambarish Nag, Michael I. Monine, Byron Goldstein, James R. Faeder and Michael L. Blinov (2012). Mathematical Modeling of Syk Activation in Allergen-Stimulated Mast Cells and Basophils, Advances in Protein Kinases, Dr. Gabriela Da Silva Xavier (Ed.), ISBN: 978-953-51-0633-3, InTech, Available from: http://www.intechopen.com/books/advances-in-protein-kinases/mathematical-modeling-of-syk-activation-in-allergen-stimulated-mast-cells-and-basophils

INTECH
open science | open minds

InTech Europe
University Campus STeP Ri
Slavka Krautzeka 83/A
51000 Rijeka, Croatia
Phone: +385 (51) 770 447
Fax: +385 (51) 686 166
www.intechopen.com

InTech China
Unit 405, Office Block, Hotel Equatorial Shanghai
No.65, Yan An Road (West), Shanghai, 200040, China
中国上海市延安西路65号上海国际贵都大饭店办公楼405单元
Phone: +86-21-62489820
Fax: +86-21-62489821

IntechOpen